Chemical Geology xxx (2008) xxx–xxx

Contents lists available at ScienceDirect

Chemical Geology

journal homepage: www.elsevier.com/locate/chemgeo

Nb and Zr behavior in rutile during high-grade metamorphism and retrogression: An example from the Ivrea–Verbano Zone

G.L. Luvizotto *, T. Zack

Mineralogisches Institut, Universität Heidelberg, Im Neuenheimer Feld 236, 69120 Heidelberg, Germany

ARTICLE INFO

Article history:
Accepted 29 July 2008
Available online xxxx

Keywords:
Accessory phases
Trace element
Partitioning
Slow cooling
Diffusion
Fluids

ABSTRACT

Detailed textural observations and in situ analyses (EMP, SIMS and LA-ICP-MS) are used to characterize trace element behavior during prograde and retrograde metamorphic reactions involving rutile. The Ivrea–Verbano Zone is a classic granulite area and rocks from the Strona and d'Ossola valleys are an example of the amphibolite to granulite facies transition. Although different rock types occur in the area, detailed sampling and petrographic work show that rutile only occurs in granulite facies paragneisses. These rocks show a rich inventory of textures that allow not only for the investigation of trace element behavior in response to prograde rutile growth, but also for the effect of post-peak processes on rutile chemistry. Nb concentrations in rutile from lower grade samples show a larger spread (from 500 to 5000 ppm within one sample) when compared to those from higher grades. This pattern can be modeled using prograde rutile growth formed from biotite breakdown. Zr concentrations in rutile are characterized by an anomalously large spread and a bimodal distribution. Maximum Zr concentrations increase according to the general metamorphic gradient known for this area. Temperatures (from Zr-in-rutile thermometry), although feasible, are considerably higher than previous calculations (increasing from ca. 850 to 930 °C). A second cluster of Zr concentrations in rutile occurs at rather constant concentrations (ca. 1000 ppm) for all localities and is interpreted to be related to intense fluid influx at high-temperature and/or to post-peak diffusional resetting favored by slow cooling rates. Alteration textures, characterized by a complex network of micro-veins, are evidence for the late fluid influx. The fluid strongly affected the rutiles, which is evidenced by corrosion of older rutile grains and formation of rutile veinlets.

1. Introduction

Despite the relative fluid immobility of high field strength elements (HFSE; e.g., Zr, Nb, Sn, Sb, Hf, Ta, W) under subsolidus conditions (e.g., Pearce and Cann, 1973), unequivocal evidence for their mobility on a thin section scale (e.g., Zack et al., 2004a; Rasmussen, 2005; Gao et al., 2007) has sparked intense research on the behavior of HFSE distribution in metamorphic environments. Most of these efforts involve the calibration and evaluation of HFSE thermometers in the system Ti–Zr–Si–O (Zr-in-rutile or rutile thermometry, Ti-in-zircon, Ti-in-quartz, Zr-in-titanite; Zack et al., 2004a; Zack and Luvizotto, 2006; Watson et al., 2006; Wark and Watson, 2006; Tomkins et al., 2007; Hayden et al., 2007; Miller et al., 2007). Furthermore, applications to provenance studies have been realized by coupling the rutile thermometer with Nb–Cr source characteristics (Zack et al., 2002, 2004b; Stendal et al., 2006; Triebold et al., 2007; Meinhold et al., 2008). With several areas of HFSE behavior in metamorphic environments virtually unexplored, we have focused this study on the response of HFSE in rutile forming reactions in granulite facies rocks using samples from the Ivrea–Verbano Zone (IVZ) as a test case.

Rutile is a frequent HFSE phase, occurring as an accessory mineral in a wide range of rocks, i.e., high-grade metamorphic rocks, igneous rocks, siliciclastic sediments, placer deposits and hydrothermal ore deposits. It is widely known that rutile is an important carrier for several highly charged trace elements (Graham and Morris, 1973; Haggerty, 1991; Deer et al., 1992; Smith and Persil, 1997; Rice et al., 1998). For example, Zack et al. (2002) has shown for eclogites that 1 modal% of rutile can carry more than 90% of the whole rock content for Ti, Nb, Ta, Sb and W and considerable amounts (5–50% of the whole rock content) of V, Cr, Mo and Sn. It has recently been shown that the Zr incorporation in rutile in quartz- and zircon-bearing systems is strongly temperature dependent (Zack et al., 2004a; Watson et al., 2006; Tomkins et al., 2007). Rutile has also been shown to yield precise U–Pb ages (e.g. Mezger et al., 1989; Davis, 1997; Mezger et al., 1993; Li et al., 2003; Vry and Baker, 2006).

The Ivrea–Verbano Zone is one of the world's classic granulite facies areas and has been the subject of study for several decades (e.g., Berckhemer, 1969; Schmid and Wood, 1976; Zingg, 1980, 1983; Zingg et al., 1990; Sills and Tarney, 1984; Schmid et al., 1987; Boriani et al., 1990; Vavra et al., 1996; Rivalenti et al., 1997; Barboza et al., 1999; Vavra and Schaltegger, 1999; Barboza and Bergantz, 2000; Peressini et al., 2002, 2007; Rutter et al., 2007). The area is also a textbook example of the amphibolite granulite facies transition and its associated processes (e.g.,

* Corresponding author.
E-mail address: gluvizot@min.uni-heidelberg.de (G.L. Luvizotto).

0009-2541/$ – see front matter © 2008 Elsevier B.V. All rights reserved.
doi:10.1016/j.chemgeo.2008.07.023

dehydration melting and melt loss). The IVZ is, therefore, an excellent site to investigate the interplay between metamorphism, cooling, diffusion and trace element distributions during metamorphic reactions.

The aim of the present study is to characterize, through detailed textural observations and in situ analyses, the behavior of HFSE elements during prograde and retrograde reactions involving rutile.

2. The Ivrea–Verbano Zone

2.1. Geological setting

The Ivrea–Verbano Zone (Fig. 1) in the Southern Alps is one of the best preserved sections through lower continental crust. It is delimited to the northwest by the Insubric Line, a major Neogene shear zone that juxtaposes pre-Alpine and Alpine structures and rocks (Schmid et al., 1987). To the southeast, the boundary of the IVZ is tectonically delimited by the Cossato–Mergozzo–Brissago tectonic discontinuity (Boriani et al., 1990). The metamorphic foliation and primary banding are mostly steeply dipping and show a NE–SW trend, parallel to the Insubric Line. The area is traditionally divided into two main units: a large basic intrusive complex of Permian age (the Mafic Formation of Zingg, 1980; Rivalenti et al., 1981, among others) and a sequence of metasedimentary rocks interlayered with bands of mafic rocks (see Fig. 1).

Rocks, occurring in the area comprised by the Strona and d'Ossola valleys, show a metamorphic gradient with metamorphic conditions increasing from amphibolite facies in the southeast, to granulite facies in the northwest. Zingg (1980) mapped two important mineral isograds (see location in Fig. 1): the muscovite-out/K-feldspar-in in metapelitic rocks and the orthopyroxene in mafic and intermediate rocks. In most models, the increase of metamorphic grade from southeast to northwest together with the steep foliation and primary banding has been interpreted to be the result of an Alpine-age tilting of the IVZ, and hence exposing a cross-section through the lower continental crust (e.g., Handy et al., 1999; Rutter et al., 2007). Although the metamorphic grade increases more or less continuously, it has to be stressed that significant post-peak metamorphic shearing and folding is observed (Rutter et al., 2007).

Pressure (P) and temperature (T) estimates of the IVZ have been presented by various authors (Zingg, 1980; Sills and Tarney, 1984; Henk et al., 1997; Demarchi et al., 1998; Barboza and Bergantz, 2000, among others).

Maximum PT conditions calculated by Henk et al. (1997) are 810 °C and 0.83 GPa and decrease to 710 °C and 0.67 GPa towards the granulite to amphibolite facies boundary.

The heat source for the regional granulite facies metamorphism has long been a subject of debate in the literature. It has traditionally been attributed to the intrusion of the mafic rocks of the Mafic Formation (Zingg, 1980; Zingg et al., 1990). Recently, Peressini et al. (2007) presented geochronological data on the duration of the mafic intrusion. The authors allocated an age of ~310 Ma ($^{206}Pb/^{238}U$ zircon ages) to a Carboniferous orogenic event that affected the metasedimentary rocks (see also Köppel, 1974; Vavra et al., 1996; Henk et al., 1997). One of the main conclusions of Peressini et al. (2007) is that the granulite grade metamorphism affected the metasedimentary rocks about 20 Ma before the crystallization of the Mafic Complex. Their observations are in agreement with the previous findings of Barboza et al. (1999) and Barboza and Bergantz (2000), who inferred that the granulite facies metamorphism preceded the emplacement of the Mafic Complex. Peressini et al. (2007) presented a detailed investigation on the heat transfer caused by the intrusion of the Mafic Complex. They concluded

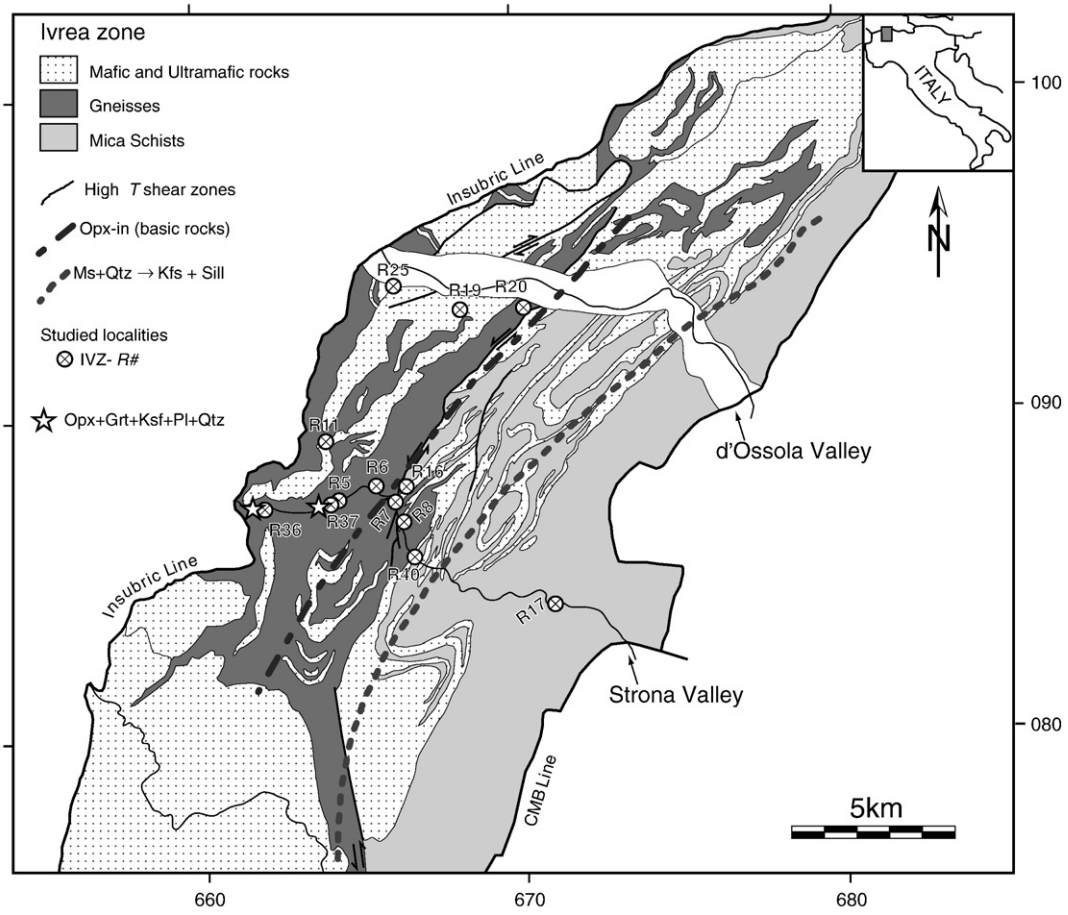

Fig. 1. Geological map of the central part of the IVZ. Redrawn and simplified from Rutter et al. (2007). Main metamorphic isograds are those presented by Zingg (1980). CMB Line=Cossato–Mergozzo–Brissago Shear Zone.

Please cite this article as: Luvizotto, G.L., Zack, T., Nb and Zr behavior in rutile during high-grade metamorphism and retrogression: An example from the Ivrea–Verbano Zone, Chemical Geology (2008), doi:10.1016/j.chemgeo.2008.07.023

that the thermal anomaly caused by the intrusion lasted several million years. This leads to the conclusion that the post-intrusion tectonic evolution of the IVZ rocks is characterized by distinctly slow cooling rates.

As rutile is the main focus of our research, we carried out detailed sampling and petrographic work in order to evaluate its occurrence in the IVZ rocks. Investigation of more than 60 thin sections derived from 38 localities within the area of the Strona and d'Ossola valleys by petrographic microscope, BSE imaging and EDS analyses led to the identification of six main rock types: K-feldspar and sillimanite bearing gneisses (Grt+Sil+Kfs+Qtz+Rt±Pl±Bt; mineral abbreviations after Kretz, 1983), strongly restitic sillimanite bearing and garnet-rich (up to 70%) gneisses (Grt+Sil+Qtz+Pl+Rt±Kfs±Bt), mafic rocks (Amph+Pl+Ilm±Qtz±Cpx±Grt; Grt+Opx+Pl+Ilm±Amph±Qtz±Cpx), plagioclase-rich and sillimanite-free gneisses (Grt+Pl+Kfs+Qtz+Ilm±Opx±Bt), garnet–sillimanite micaschists (Grt+Bt+Sil+Qtz±Ms±Pl) and calcsilicate rocks (Cal+Cpx+Scp+Ttn±Qtz±Pl). Our findings are in agreement with results reported by Zingg (1980) and show that rutile is only present in the granulite facies paragneisses also know in the literature as "stronalite".

2.2. Critical evaluation of PT conditions from former studies

As previously stated, several *PT* estimates are available in the literature for the IVZ rocks. However, they are all based on Fe–Mg exchange thermometers (garnet–biotite, garnet–orthopyroxene). Various studies have shown that temperatures calculated using these thermometers may be underestimated due to Fe-Mg exchange from cooling after peak metamorphic conditions and, therefore, the results must be corrected for this late exchange (Harley, 1989; Fitzsimons and Harley, 1994; Pattison and Begin, 1994; Pattison et al., 2003). For example, Pattison et al. (2003) have shown that the amphibolite to granulite facies transition (defined by mineral associations in metapelitic rocks developed at *PT* conditions analog to the appearance of orthopyroxene in mafic and intermediate compositions) occurs at temperatures of about 850 °C and are therefore significantly higher than those determined for the IVZ.

Despite calculating absolute temperatures with Fe–Mg exchange thermometry, which is prone to diffusional resetting; imprecise, but robust *PT* estimates can be made with the typical granulite facies mineral assemblage in the IVZ: Grt+Kfs+Sil+Rt±Pl±(+liq). In the simplified system NaKFMASH presented in Fig. 2, the shaded area represents the stability field for the mineral assemblage which is bounded by the reactions Bt+Sil=Grt+Crd+liq on the low pressure side, Sil=Ky on the high pressure side and for high-Mg bulk compositions Bt+Grt=Opx+Sil+liq on the high-temperature side. Minimum temperatures are given by the reaction Bt+Sil=Grt+Kfs+liq. With Fe/(Fe+Mg) ratios of 0.6–0.8 in garnets from such samples (Schmid and Wood, 1976; Henk et al., 1997), a minimum temperature of ca. 780 °C can be designated. The incorporation of Ti shifts the stability of biotite to higher *T* conditions (Patiño-Douce, 1993; Patiño-Douce and Beard, 1995; Dooley and Patiño-Douce, 1996; Henry and Guidott, 2002; Henry et al., 2005) for the reaction Bt+Grt=Opx+Sil+liq by ca. 40 °C (White et al., 2007).

The mineral assemblage Opx+Grt+Kfs+Pl+Qtz in metagraywackes has been recorded in a few localities near Forno (Sills, 1984, see also Fig. 1 for location and Fig. 3 for BSE image). This mineral assemblage is bounded at lower temperature (ca. 800 °C at 0.7 GPa) by the reaction Bt+Pl+Qtz=Opx+Ksp+liq (see Fig. 2).

In summary, temperature conditions for the rutile-bearing samples in the IVZ can be estimated from phase mineral assemblages to be between ca 770 °C to 940 °C at 0.6 to 1.0 GPa, probably with a general increase in metamorphic grade from the southeast to the northwest.

3. Analytical techniques

3.1. Electron Microprobe (EMP)

Electron microprobe studies were carried out at the Mineralogisches Institut, Universität Heidelberg using a CAMECA SX51 equipped with 5 WDS detectors. Analyses of rutiles were carried out with 20 kV and 100 nA and followed the method outlined by Luvizotto et al. (this issue). The following elements were analyzed: Si, V, Cr, Fe, Zr, Nb and W. With

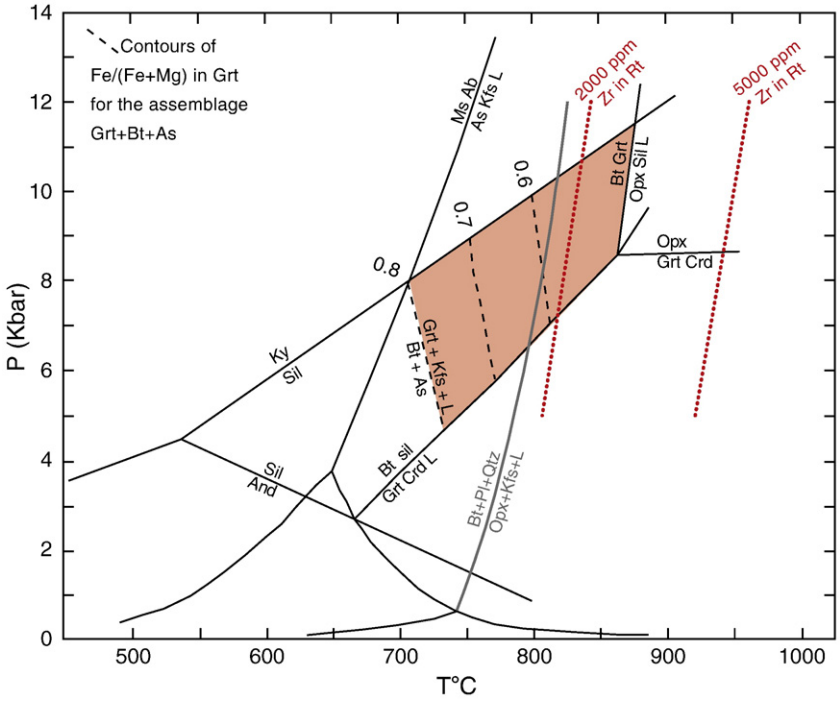

Fig. 2. Minimum *PT* estimates for the granulite facies rocks from IVZ. Solid lines represent main reactions for the NaKFMASH system Spear et al. (1999). The position of the Bt+Pl+Qtz=Opx+Kfs+liq reaction (stippled lines) is from Spear (1995). Shaded area represents the stability field for the paragenesis present in the granulite facies metapelitc rocks from the IVZ. Dotted lines represent temperatures calculated using the Zr-in-Rt thermometer (calibration of Tomkins et al., 2007) for the maximum concentrations recorded in IVZ samples.

Please cite this article as: Luvizotto, G.L., Zack, T., Nb and Zr behavior in rutile during high-grade metamorphism and retrogression: An example from the Ivrea–Verbano Zone, Chemical Geology (2008), doi:10.1016/j.chemgeo.2008.07.023

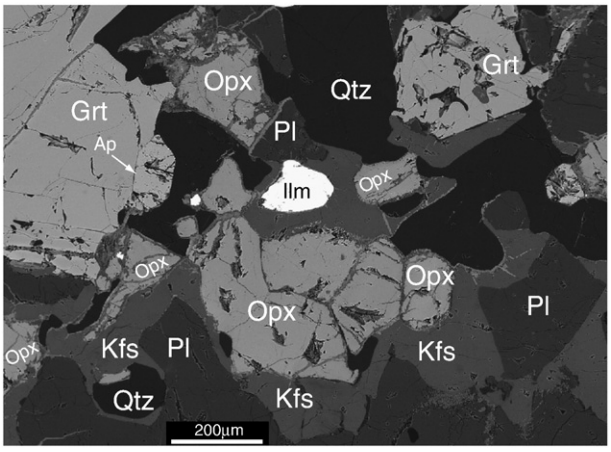

Fig. 3. BSE image example of the mineral assemblage Opx + Grt + Kfs + Pl + Qtz in a plagioclase-rich sillimanite-free gneiss from the Strona Valley. Note that this rock is rutile-free.

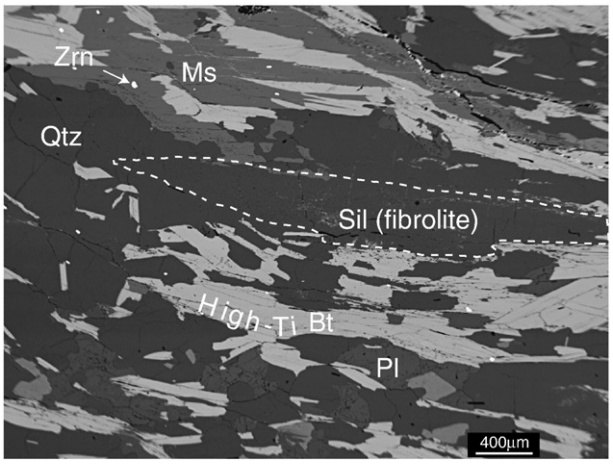

Fig. 4. BSE image example of the amphibolite facies micaschist (IVZ-R17b). Although not shown in this figure, garnet may also be present. In these rocks, the main Ti-carrier is the High-Ti Bt (up to 7.00 wt.% TiO_2).

the chosen setup, the detection limits (2σ) are 50 ppm for Cr, 40 ppm for Fe and Zr, 60 ppm for Nb and 350 ppm for W and the 2σ relative standard errors are 20 ppm for Cr and Fe, 40 ppm for Zr, 60 ppm Nb and 90 ppm W. In order to get "true" zero-concentration peak intensities and to exclude any machine drift, every ten analyses of unknowns were bracketed by two analyses of synthetic rutile (nominally zero-concentration trace elements). Si concentrations were used as a quality control to detect and avoid contamination associated with submicroscopic zircon inclusions (according to the method outlined by Zack et al., 2004a). Rutile measurements with Si concentrations higher than 300 ppm that showed abnormally high Zr contents were excluded from the data set. Measurements with Si content slightly above 300 ppm and Zr concentrations similar to rutiles with low Si contents were included for small (20–30 µm) rutile grains (high Si values were interpreted to be related to the surrounding silicates). The same quality controls are applied to SIMS and LA-ICP-MS analyses. In total, less than 2% of the measurements had to be discarded due to contamination. Although the EMP beam's diameter was set to 5 µm, the minimum grain size for obtaining reliable analyses was 20 µm.

3.2. Secondary Ion Mass Spectrometry (SIMS)

SIMS analyses were carried out at the Mineralogisches Institut, Universität Heidelberg using a CAMECA ims 3f. Analyses were performed using a 14.5 keV/10–20 nA $^{16}O^-$ primary ion beam, which resulted in spot sizes of 20–30 µm. However, by using a field aperture the effective spot size could be reduced to 12 µm, leading to the smallest analyzable grain sizes of 20–30 µm. Positive secondary ions were nominally accelerated to 4.5 keV (energy window set to ±20 eV) and the energy filtering technique was used with an offset of 90 eV at mass resolution $m/\delta m$ (10%) of 370. Count rates were normalized to ^{47}Ti. TiO_2 in rutile is assumed to be 100 wt.%. The following isotopes were analyzed: ^{27}Al, ^{30}Si, ^{47}Ti, ^{90}Zr, ^{93}Nb, ^{118}Sn, ^{120}Sn, ^{121}Sb, ^{123}Sb, ^{178}Hf, ^{181}Ta, ^{184}W, ^{186}W, ^{232}Th, ^{238}U. Results obtained for the two isotopes analyzed for Sn, Sb and W do not display any systematic differences, showing that no mass interference affected these isotopes in rutile analyses by SIMS (for further discussion see Luvizotto et al., this issue). Therefore, concentrations presented in Appendix A represent the average of the values obtained for the two measured isotopes. Concentrations were calculated based on relative sensitivity factors (RSF) obtained from the rutile R10 (Luvizotto et al., this issue). Although no reliable RSF can be calculated for Th, the intensity ratios obtained for the studied rutiles suggest that Th concentrations are extremely low (below the 0.1 ppm level when using RSF from U). SIMS analyses carried out on some biotite grains followed the procedure described above.

Table 1
Summarized description of the rutile-bearing granulite facies gneisses

Locality	Thin sec.	Valley	Coordinates		Late alter.	Qtz	Grt	Sil	Bt	Kfs	Pl	Rt	Zrn	Ilm
			E	N										
IVZ-R7	a	Strona	444899	5086949	H	xx	x	xx	2–3%	xx	–	<1%	<1%	
IVZ-R16[a]	a	Strona	445276	5087496	M-L	xx	xx	I	3%	xx	–	2%	<1%	
	f				M	x	xx	xx	7%	xx	–	<1%	<1%	
	g				M	xx	x	–	5%	I	xx	<1%	<1%	
IVZ-R6	b	Strona	444327	5087510	M	I	xx	x	<1%	–	x	2–3%	<1%	
IVZ-R5	b	Strona	443321	5087041	H	xx	x	x	5%	x	–	<1%	<1%	
IVZ-R37	b	Strona	443504	5086997	M	x	xx	–	<1%	I	x	2%	<1%	<2%[b]
IVZ-R36	a	Strona	440850	5086389	M-L	xx	x	x	<1%	I	x	2%	<1%	
	g[c]				M-L	xx	x	x	<1%	I	x	2%	<1%	
IVZ-R11		Between	442376	5088973	H	xx	xx	–	3%	x	x	1%	<1%	
IVZ-R20	a	d'Ossola	449102	5092801	M-H	x	x	xx	<1%	xx	–	3%	<1%	
	j				M-L	xx	xx	I	2%	x	x	1%	<1%	
IVZ-R19	e	d'Ossola	447111	5092780	L	X	xx	xx	3%	x	x	1%	<1%	
IVZ-R25	b	d'Ossola	445116	5096942	M	X	xx	xx	<1%	I	xx	2%	<1%	

Modal proportions are based on visual inspection with a petrographic microscope and BSE images.
Modal proportion: I — 1 to 10%, x — 10 to 20%, xx — >20%. Intensity of the late alteration (Late alt.): high (H), medium (M) and low (L). Coordinates are presented in UTM (WGS84).
[a] Banded gneiss with portions rich in Kfs + Sil (R16a), portions slightly richer in Bt (R16f) and portions rich in Pl (R16g).
[b] Included in Grt core and alteration product of Rt.
[c] Collected ~40 m north (higher metamorphic grade) of IVZ-R36a.

Please cite this article as: Luvizotto, G.L., Zack, T., Nb and Zr behavior in rutile during high-grade metamorphism and retrogression: An example from the Ivrea–Verbano Zone, Chemical Geology (2008), doi:10.1016/j.chemgeo.2008.07.023

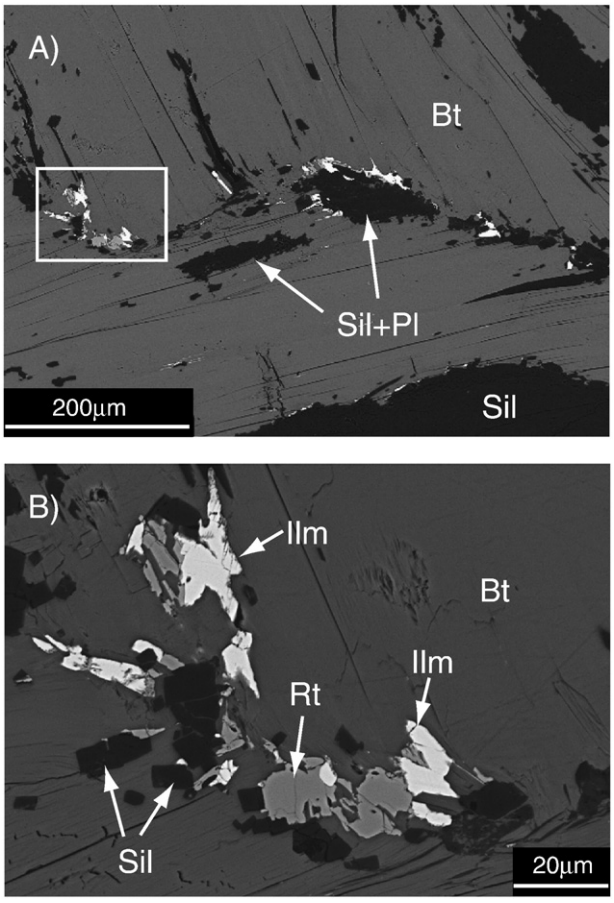

Fig. 5. BSE images showing examples of small rutile and ilmenite grains found in high amphibolite facies Grt-Sil-Bt schists from the IVZ (sample IVZ-R40c). The white rectangle delimits the close-up in B.

3.3. Laser Ablation Inductively Coupled Plasma Mass Spectrometry (LA-ICP-MS)

Trace element analyses were carried out at the Institut für Geowissenschafent, Johannes Gutenberg-Universität Mainz, using a New Wave Research UP-213 (wavelength 213 nm) laser system combined with an Agilent 7500ce ICP quadrupole mass spectrometer. Analyses followed the procedures presented by Luvizotto et al. (this issue). Element concentrations were calculated with the software "GLITTER" using the measurements of the following isotopes: ^{90}Zr, ^{93}Nb, ^{177}Hf, ^{178}Hf, ^{181}Ta, ^{238}U. Typical detection limits (99% confidence) for 70 μm spots are 0.01 ppm for Zr and Hf, 0.005 ppm for Nb and 0.004 ppm for Ta and U.

LA-ICP-MS analyses were carried out on rutiles and biotites from sample IVZ-R19 in order to investigate how Nb and Ti partition between these minerals and to confirm results obtained by SIMS.

3.4. X-Ray Fluorescence (XRF)

Bulk-rock chemical concentrations were obtained by XRF analyses at Universität Heidelberg using a SRS 300 wavelength-dispersive spectrometer (Bruker AXS). Major and trace elements were determined using pressed powder tablets. International reference materials were used for the calibration.

4. Results

In this section, we present the trace element composition of the studied rutiles, focusing on Zr and Nb. The samples derived from 10 different localities within the area of the Strona and d'Ossola valleys (Fig. 1). Key information of the studied rocks is presented in Table 1. A table including concentration data for all analyzed elements is presented in Appendix A.

4.1. Microtextural observations of rutile and other Ti-bearing phases

In the studied area, the appearance of rutile is associated with the amphibolite to granulite facies transition. Amphibolite facies micaschists are rutile-free and biotite is the main Ti-carrier (up to 7.00 wt.% TiO_2). Fig. 4 shows a BSE image of this rock. The transition is associated to a sequence of dehydration reactions first involving muscovite (to form sillimanite and potassic feldspar) and then biotite (to form garnet and potassic feldspar). The Ti released by the breakdown of biotite leads to rutile formation, which can be described by the reaction: (high-Ti) Bt + Sil + Qtz = Grt + Kfs + Rt + Melt (see also Zingg, 1980).

The metamorphic textures support the theory of rutile formation associated with the biotite breakdown. For example, in some samples from the upper-amphibolite facies (garnet–biotite–sillimanite schist), small (~20 μm) rutile and ilmenite grains are present. The grains occur preferentially along biotite rims and within cleavage planes (Fig. 5). In the granulite facies rocks, rutile occurs as large grains (often larger than 100 μm) in the matrix and included in garnet (preferentially at the rim) indicating synmetamorphic crystallization of rutile and garnet (Fig. 6). In addition, only a few relict biotite grains occur in these rocks and are mostly present as rounded inclusion in garnets.

Although some ilmenite grains occur together with rutile in some upper-amphibolite facies rocks (Fig. 5), the paragenesis (metamorphic equilibrium) rutile + ilmenite is not observed in granulite facies rocks.

The studied rocks are clearly affected by a post-peak alteration that is evidenced by a complex network of micro-veinlets that affect virtually all mineral phases, including rutile. Although frequent, the intensity of the alteration varies from sample to sample (a classification is given in Table 1). Fig. 7 shows BSE images exemplifying how these infiltrating

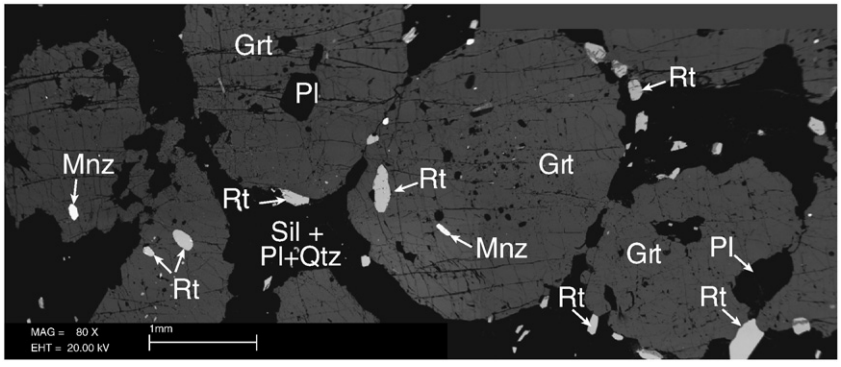

Fig. 6. BSE image showing a texture observed in granulite facies restitic rocks from the IVZ (sample IVZ-R6b). Note that large rutile grains are only present in the matrix and in the garnet rims.

Please cite this article as: Luvizotto, G.L., Zack, T., Nb and Zr behavior in rutile during high-grade metamorphism and retrogression: An example from the Ivrea–Verbano Zone, Chemical Geology (2008), doi:10.1016/j.chemgeo.2008.07.023

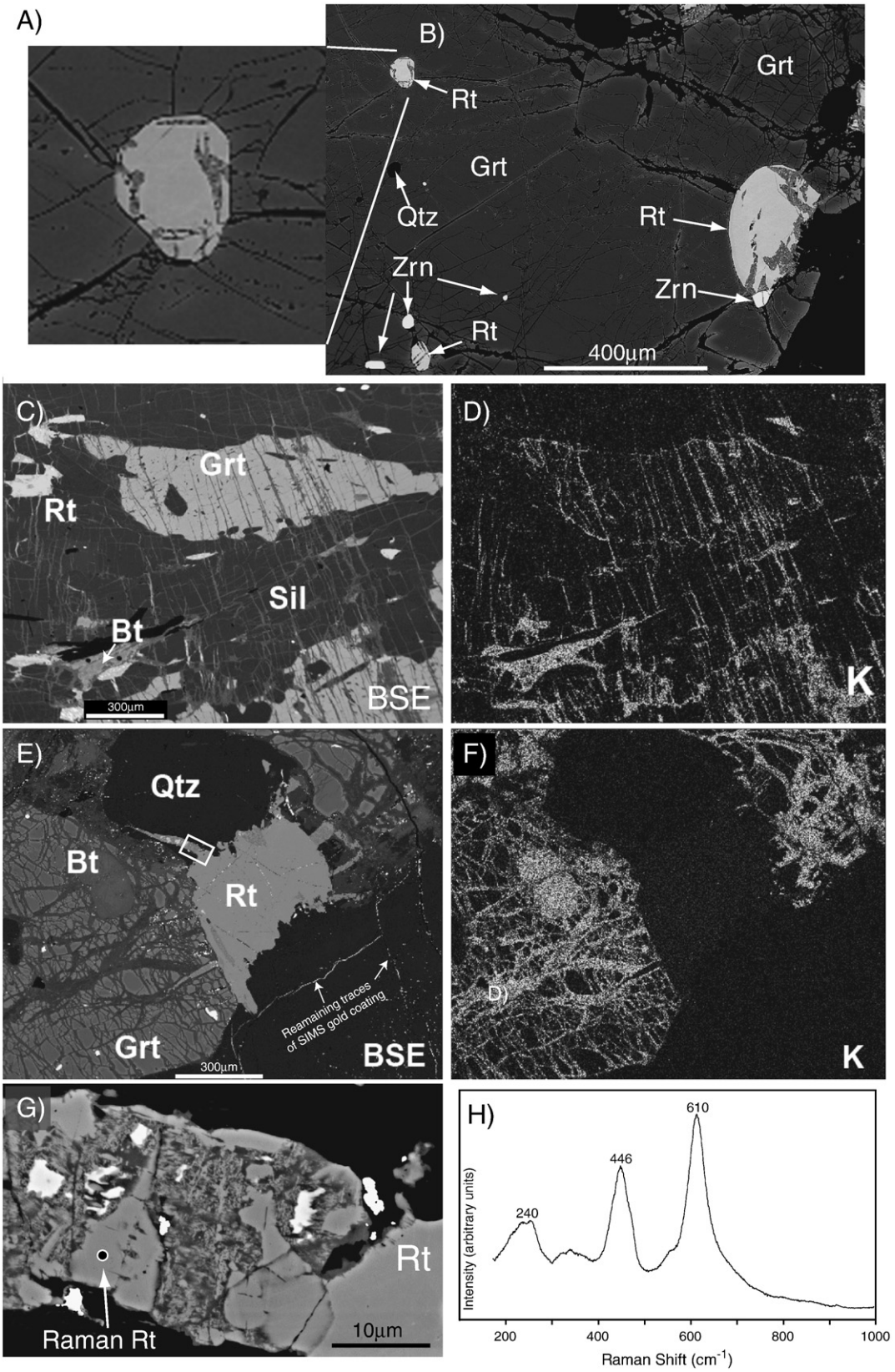

Fig. 7. BSE image examples of the post-peak veins present in the granulite facies rutile-bearing rocks. Note how the veins affect not only the rock-forming minerals but also the rutiles, even those included in garnet (detail in (A)). Chemical maps presented in (D) and (F) correspond to the same areas shown in (C) and (E) and were obtained by EDS. Higher concentrations are represented by brighter colors. Zircons in contact with rutile, such as the example given in (B), are frequently observed. (G) shows an enlargement of the rutile veinlet observed in (E) showing location of the Laser Raman spot (the spectrum is displayed in (H)). Samples: B — IVZ-R16a, C — IVZ-R20a, E — IVZ-R11.

Please cite this article as: Luvizotto, G.L., Zack, T., Nb and Zr behavior in rutile during high-grade metamorphism and retrogression: An example from the Ivrea–Verbano Zone, Chemical Geology (2008), doi:10.1016/j.chemgeo.2008.07.023

fluids chemically altered the minerals. The veins are composed of very fine crystallized phases (too small for the in situ analyses used in this study) with a platy habit. As shown in the chemical maps presented in Fig. 7D and F, they are characterized by a high K content. In Fig. 7B veins cut through garnet crystals indicating that the fluids were able to chemically alter the garnet composition (brighter colors closer to the rims of the cracks). Even rutiles included in garnets (see detail in Fig. 7A) are affected by fluids inferred to have accessed the rock via the vein system now observed within it. The late alteration affected the rutiles in two ways. Large, granulite facies rutile grains often show corroded rims and internal alterations that follows the orientation of the veins. In rutiles, the alteration product is characterized by a patchy distribution of very fine-grained material composed of rutile, ilmenite, titanite and a fine-grained platy material, probably chlorite. A second, and notable texture, shows that the alteration was coupled with crystallization of anhedral rutile veinlets along the veins (Fig. 7E and G). Rutile was identified by Raman bands at 245, 446 and 610 cm−1 (Fig. 7H, for a compilation of Raman bands for Ti polymorphs see Meinhold et al., 2008). To our knowledge such rutile veinlets have not been described in the literature. This texture implies substantial local remobilization of Ti.

4.2. Zirconium concentrations in rutile

Zirconium concentrations in rutiles from the IVZ rocks are characterized by an anomalously large spread, varying from less than 700 to more than 5000 ppm (Fig. 8, for a complete data set refer to Appendix A). As the Zr incorporation in rutile is temperature dependent (Zack et al., 2004a; Watson et al., 2006; Tomkins et al., 2007) and granulite facies rocks are usually well equilibrated due to the high temperatures, these results are rather unexpected. Furthermore, such a large spread in concentration has so far not been reported in other metamorphic rocks (Zack et al., 2004a; Zack and Luvizotto, 2006; Spear et al., 2006; Triebold et al., 2007). The only exception is greenschist facies quartzites, where the large spread of Zr concentration in rutile is probably from premetamorphic detrital relicts (Triebold et al., 2007).

In order to evaluate if the large variations observed were associated to internal zoning, rim and core analyses were carried out in some rutile grains. The results show that although some intra–grain variations occur, the inter-grain variations are much more expressive (Fig. 9). Furthermore, no relation between grain size and Zr concentration is observed. Additionally, no systematic internal variations are observed (e.g., lower concentrations at the rim of the grains). As intra-grain variations are not significant, the average concentrations obtained for the rim and the core of the grains are presented in Fig. 8.

The Zr data is often characterized by a bimodal distribution with a first cluster occurring in a rather restricted concentration range (about 1000 ppm Zr) for all samples. Interestingly, the second cluster is not always as pronounced. Still, if the localities are arranged by increasing metamorphic grade (according to what is postulated in the literature), maximum Zr concentrations increase with increasing metamorphism. This behavior is observed best in the Strona Valley (higher sampling density) where an increase of about 3000 ppm in Zr is registered from

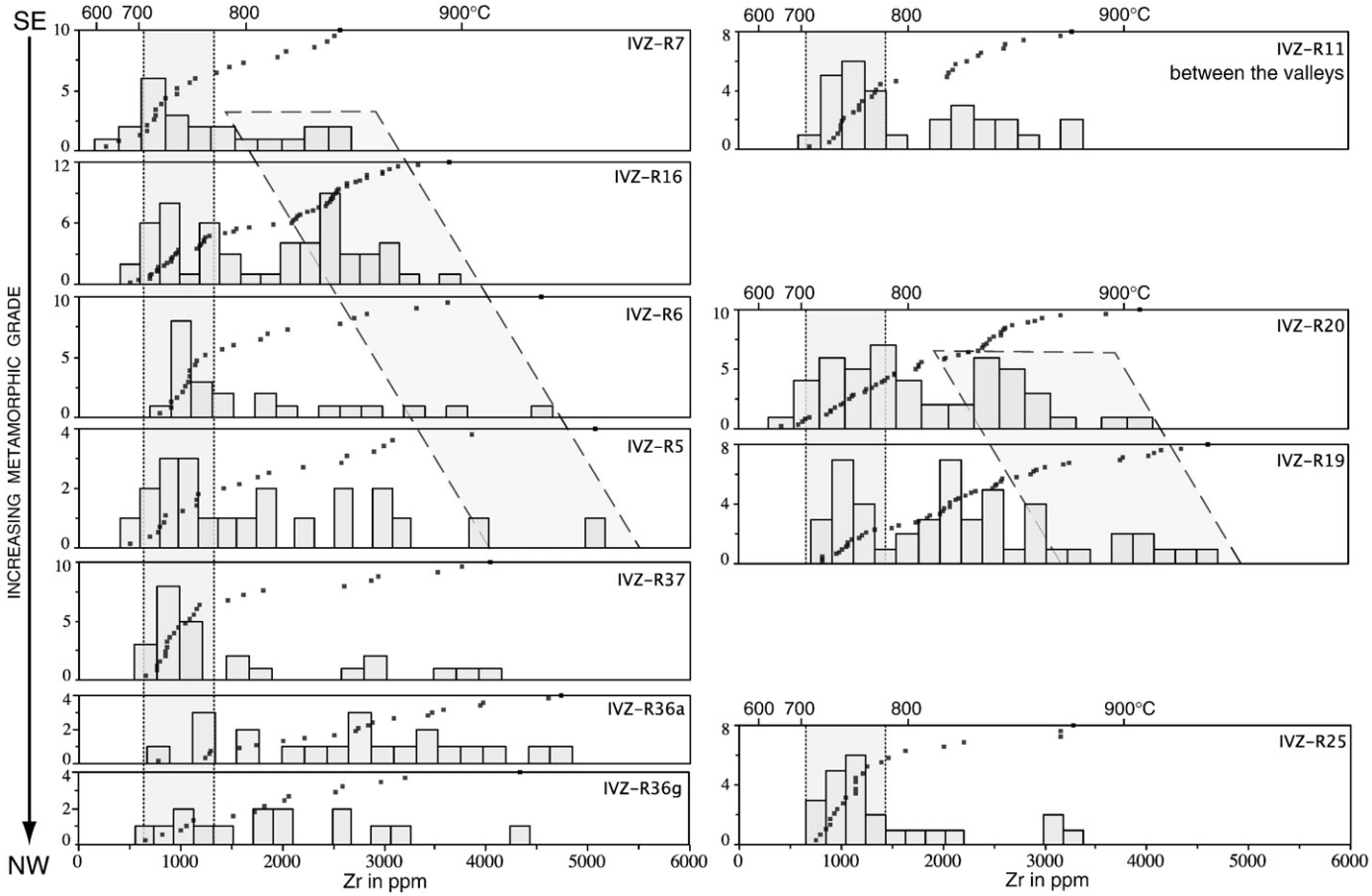

Fig. 8. Histograms showing frequencies of Zr content in rutile (in ppm) for all studied samples (grouped by locality). Dots in the diagrams represent cumulative data points (each point represents one grain). For grains with more then one analysis the average values is presented (see discussion in the text). Notably, concentration data are characterized by a large spread and often by a bimodal distribution. Localities are arranged in such a way that the distance from Insubric Line increases upwards (Fig. 1). Location IVZ-R11 is between the river sections. Sample IVZ-R36g was collected ~40 m NW of sample IVZ-R36a and therefore is presented in a separate diagram. For grains with both EMP and SIMS analyses (total of 19 grains) only SIMS data is plotted (concentrations obtained by both techniques were always within the intra-grain variation — for a complete data set refer to Appendix A).

Please cite this article as: Luvizotto, G.L., Zack, T., Nb and Zr behavior in rutile during high-grade metamorphism and retrogression: An example from the Ivrea–Verbano Zone, Chemical Geology (2008), doi:10.1016/j.chemgeo.2008.07.023

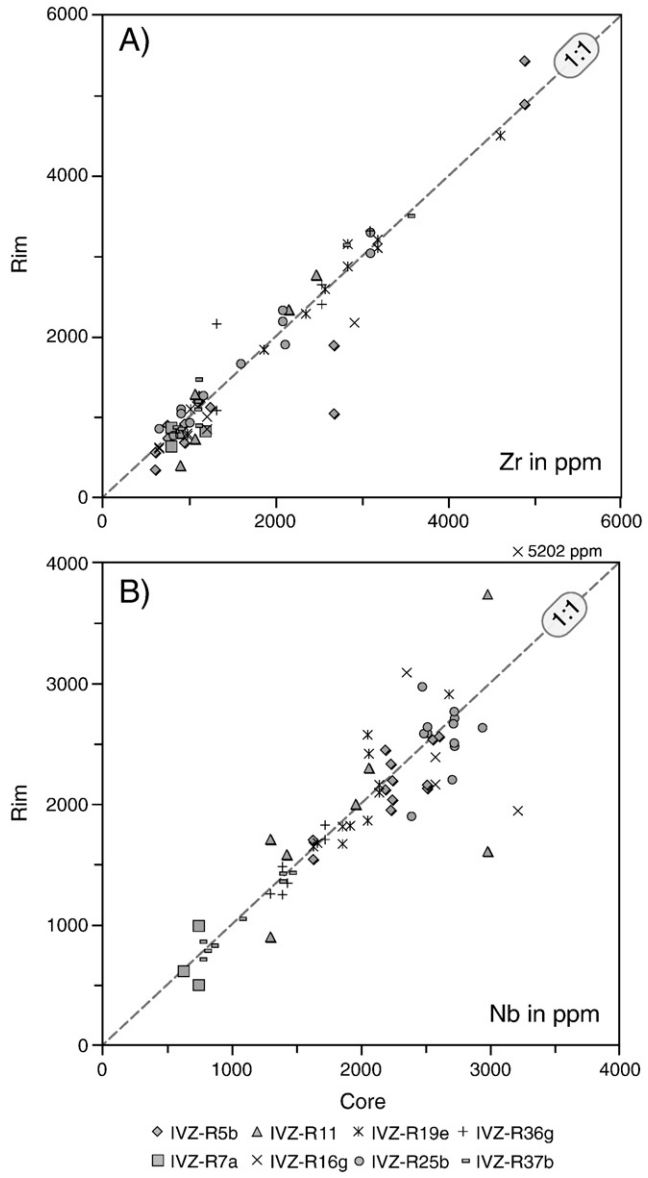

Fig. 9. Comparison of Zr and Nb concentrations obtained for the rim (~20–30 μm from the edge of the grains to avoid contamination from surrounding silicates) and the core of some rutile grains. For both Zr and Nb the inter-grain variation is much more expressive than the intra-grain.

the localities IVZ-R7 to R5 (Fig. 8). Curiously, locations expected to record the highest temperatures do not have the highest Zr concentration.

Previous work (e.g., Zack et al., 2004a; Spear et al., 2006; Triebold et al., 2007) has reported systematic differences in the Zr composition for those rutiles occurring in the matrix and those included in other phases (e.g., garnet or pyroxene). However, in our samples high Zr concentrations are not controlled by such textural relationships (matrix vs. inclusion). Examples presented in Fig. 10A–D show that rutiles with high Zr concentrations occur in contact with garnet (Fig. 10A), in the matrix (Fig. 10B) or are included in garnet (sometimes associated with cracks, Fig. 10C and D, respectively). Rather, low Zr values are preferentially obtained for rutiles that are occurring close to or in contact with zircons. Fig. 10E–H present BSE images of such textural relationships. It is noteworthy that similar observations have been presented by Harley (2008) for rutiles from the Napier Complex. Although some of the low Zr rutiles presented here show effects of the late alteration (corroded grains presented in Fig. 10E and H) the low Zr contents are not restricted to these grains (compare with Fig. 10C).

4.3. Niobium concentrations in rutile

A summary of all Nb concentrations obtained for the studied localities is presented in Fig. 11 (for a complete data set refer to Appendix A). The results show that not only does the absolute concentration range considerably (maximum variation ranging from 300 to 8800 ppm in sample IVZ-R7), but also that the spread of the values vary from locality to locality. If the data is normalized by the average and arranged according to increasing metamorphic grade, it becomes clear that the spread of the values decreases with increasing metamorphism. This trend can be observed both in the Strona and d'Ossola valley sections. As for Zr, analyses obtained at the rim and at the core of some rutile grains show that the inter-grain variations of Nb are much more pronounced than the intra-grain (Fig. 9). Systematic internal variations are also not observed for Nb.

In order to evaluate the in situ concentrations data, the results obtained for rutiles from five samples (three from the Strona and two from the d'Ossola valley) were compared to the WR data. As rutile is the main Nb and Ti-carrier, its Nb/Ti ratio should match the ratio of the WR. The comparison is presented in Fig. 12 (WR analyses are presented in Table 2). It shows that, although variation is high for some samples, the in situ results match the WR data.

It has been speculated by Zack et al. (2004b) that rutile with high Nb (>3000 ppm) may originate in biotite-bearing mineral assemblages, where biotite prefers Ti over Nb in comparison to rutile. However, this was only based on experimental phlogopite/melt partitioning data (LaTourrette et al., 1995). We therefore analyzed several biotites by LAM-ICP-MS and SIMS for HFSE (see Appendix A) in one sample (IVZ-R19e) that shows little Nb variation between different rutile grains. In this sample, relict biotite inclusions in garnet were compared with coexisting rutile (Fig. 13). Nb concentrations in biotite range between 0.34 and 4.90 ppm (average 1.9 ppm) with no observable difference between SIMS and LAM-ICP-MS analysis. With 7 wt.% TiO_2 in biotite, 100 wt.% TiO_2 and ca. 2000 ppm Nb in rutile, this confirms the prediction of a strong fractionation of the Nb/Ti ratio between rutile and biotite (ca. 50, according to the data presented by LaTourrette et al., 1995).

5. Discussion

5.1. Rutile thermometry and thermal constraints of the granulite facies metamorphism

Interpretation of the complex Zr data, with the aim of extracting temperature information for the IVZ, presents a challenge in comparison to relatively straightforward results in previous studies on natural rocks (Zack et al., 2004a; Zack and Luvizotto, 2006; Spear et al., 2006). With the absence of perfectly shielded rutile inclusions in garnet (see Fig. 7A), we are left with an open system scenario, in which rutiles have been variously affected by late resetting of their Zr content. This resetting seems to have produced a marked cluster of rutiles with Zr concentrations of about 1000 ppm (Fig. 8). This observation will be further explored in Section 5.3. Here we concentrate on the rutiles that are the least affected by this resetting, which we interpret to be represented by those towards higher Zr on the distribution diagrams presented in Fig. 8.

The calculations of apparent temperatures from Zr concentrations in rutile have been conducted using the calibration of Tomkins et al. (2007), which includes a pressure effect on the geothermometer. With the strong resetting of the Zr content, we attempt to constrain the granulite facies metamorphism by selecting the values between the 90th percentile and the maximum (values that are usually overlooked by standard statistical methods). Results are graphically presented in Fig. 14.

Please cite this article as: Luvizotto, G.L., Zack, T., Nb and Zr behavior in rutile during high-grade metamorphism and retrogression: An example from the Ivrea–Verbano Zone, Chemical Geology (2008), doi:10.1016/j.chemgeo.2008.07.023

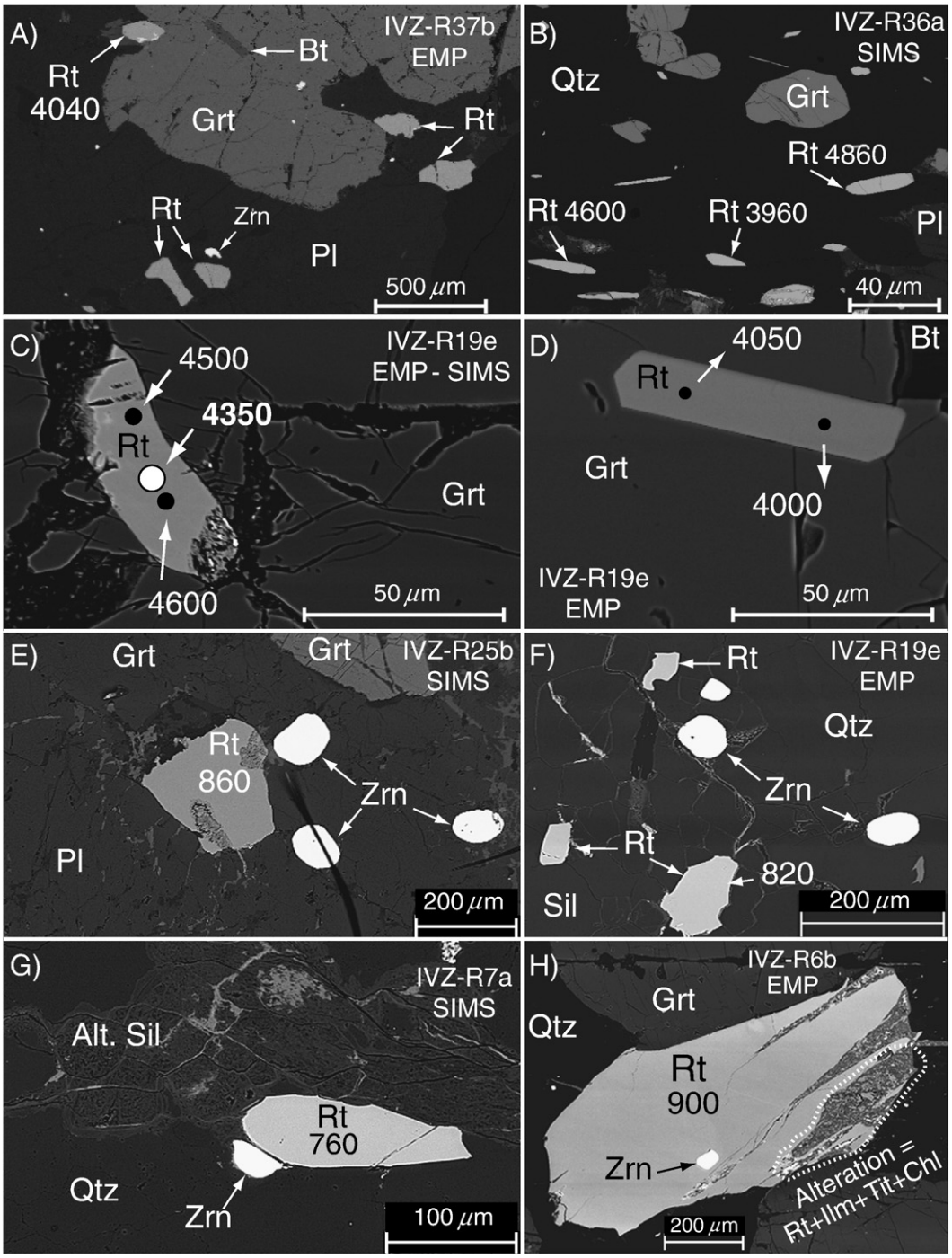

Fig. 10. BSE images showing examples of rutiles with: high Zr concentrations — A–D; and low Zr concentrations — E–H. Notice that high Zr concentrations are not controlled by textural relationships (e.g., included vs. matrix). On the other hand, low Zr contents are preferentially obtained for those rutiles that are occurring near to or in contact with zircons. Numbers correspond to Zr concentrations (in ppm) The white circle (D) represents the position of the SIMS spot (notice the agreement between EMP and SIMS results).

Temperatures calculated using the rutile thermometer are significantly higher than those previously presented in the literature, spanning from ca. 850 to 930 °C (about 100 °C higher than those obtained by Henk et al., 1997). Our data, however, point to a temperature gradient of about 80 °C within the granulite facies metapelitic rocks, which is in agreement with Henk et al. (1997). The higher temperatures obtained by the rutile thermometer are not completely unexpected, as the previously determined data were based on Fe–Mg exchange geothermometers. However, the differences are significant and the results have to be treated with caution. Preliminary results obtained by SIMS in Heidelberg show that some zircon grains from the studied samples seem also to record high temperatures, with some values above 900 °C (temperatures calculated using the Ti-in-Zrn thermometer, calibration of Watson et al., 2006). Although preliminary, these results suggest that zircon was able to form and recrystallize even at high temperatures (see also Baldwin et al., 2007; Kelsey et al., 2008).

We would like to note that overestimation of temperatures with the rutile thermometer is only possible where mineral assemblages in equilibrium with rutile are quartz-free, while underestimation can happen in zircon-absent and/or in partially reset mineral assemblages (Zack et al., 2004a; Harley, 2008). Since quartz is always present in the

Please cite this article as: Luvizotto, G.L., Zack, T., Nb and Zr behavior in rutile during high-grade metamorphism and retrogression: An example from the Ivrea–Verbano Zone, Chemical Geology (2008), doi:10.1016/j.chemgeo.2008.07.023

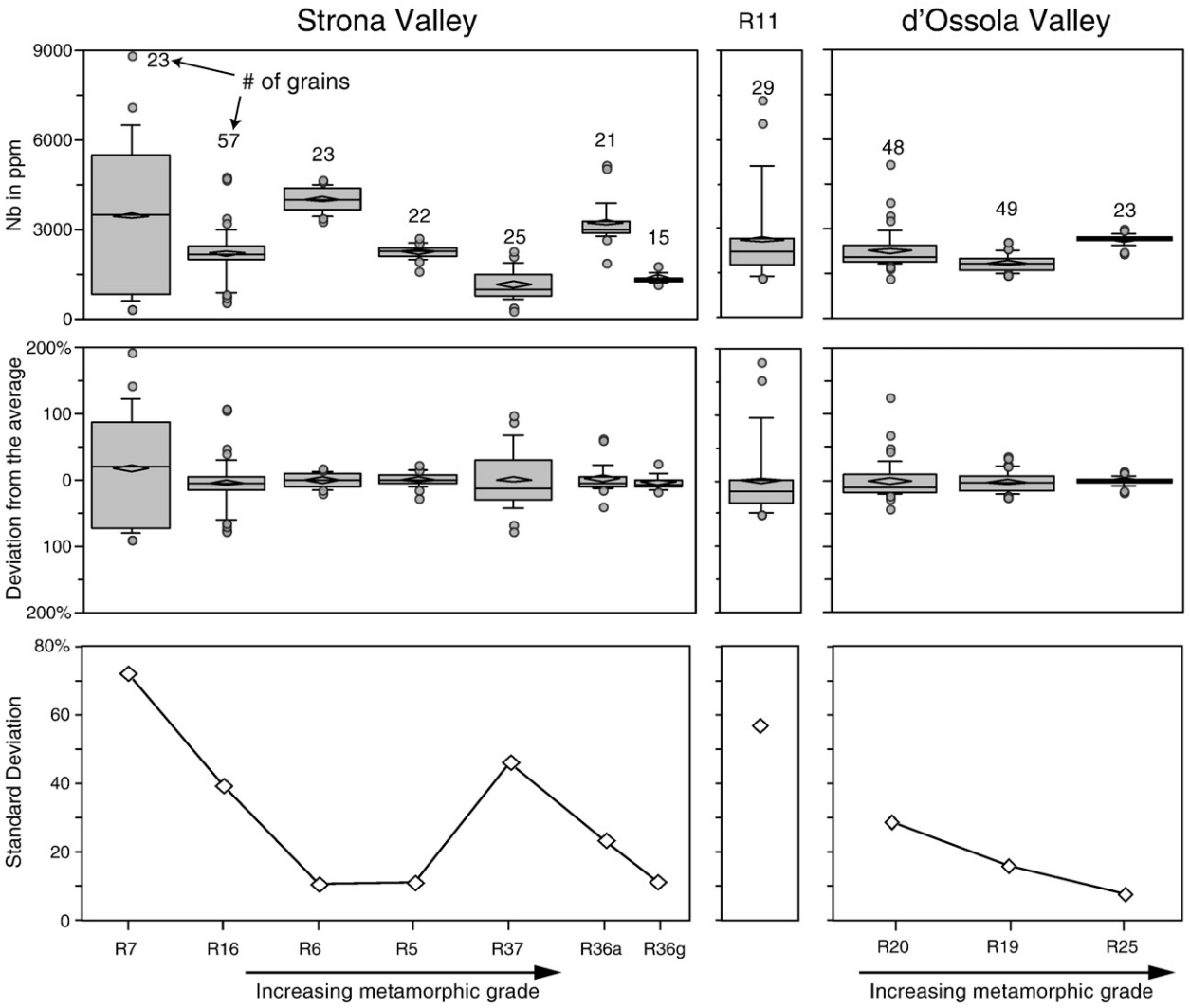

Fig. 11. Summary of Nb concentrations (EMP, SIMS and LA-ICP-MS) obtained for the studied rutiles. Samples are sorted according to increasing metamorphic grade. The boxes represent, from bottom to top, the second and third quartile (25 and 75% of the population). The bar inside the box represents the median, while the lozenge represents the average. Whiskers represent the 10th and the 90th percentile. Outliers, when they occur, are represented by small circles. The number on top of the whiskers represents the number of analyzed grains (the same for all diagrams presented in this figure). As intra-grain variations are not significant for grains with more than one analysis, average values are presented. For grains with both EMP and SIMS analyses (total of 19 grains) only SIMS data is plotted (concentrations were always within the intra-grain variation).

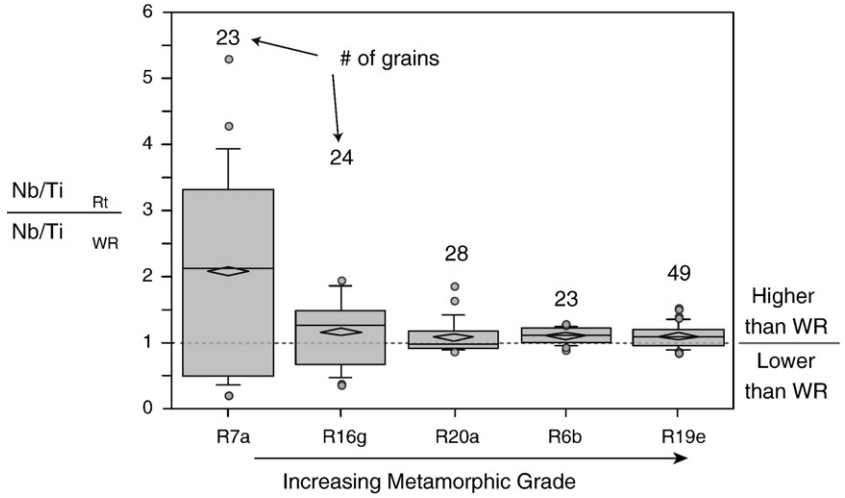

Fig. 12. Whisker and box plots (for explanation please refer to Fig. 11) summarizing Nb concentrations (EMP and SIMS) in rutiles from samples selected for WR analyses. Samples are displayed according to increasing metamorphic grade. To keep the data consistent, only rutile data from the same rock fragments analyzed for WR are presented here (therefore the number of grains differs slightly from those presented in Fig. 11).

Please cite this article as: Luvizotto, G.L., Zack, T., Nb and Zr behavior in rutile during high-grade metamorphism and retrogression: An example from the Ivrea–Verbano Zone, Chemical Geology (2008), doi:10.1016/j.chemgeo.2008.07.023

Table 2
Whole rock chemical data (XRF) obtained for selected IVZ samples

Sample	IVZ-R17B[a]	IVZ-R7A	IVZ-R16G	IVZ-R6B	IVZ-R20A	IVZ-19E
Valley	Strona	Strona	Strona	Strona	d'Ossola	d'Ossola
Peak paragenesis	Grt+Bt+Sill	Grt+Sill+Kfs+Rt	Grt+Kfs+Rt	Grt+Sill+Rt	Grt+Sill+Kfs+Rt	Grt+Sill+Kfs+Rt
SiO_2	60.9	79.2	66.7	39.9	57.3	58.1
TiO_2	1.05	0.60	0.59	2.31	1.39	1.42
Al_2O_3	20.9	9.4	15.3	27.5	22.7	21.1
$Fe_2O_3^{tot}$	9.07	5.3	6.1	18.8	11.0	11.3
MnO	0.07	0.05	0.10	0.23	0.15	0.11
MgO	2.53	1.12	2.46	5.22	2.94	2.86
CaO	0.23	0.21	3.65	4.03	0.68	0.45
Na_2O	0.62	0.29	2.75	1.00	0.68	0.39
K_2O	3.75	1.17	0.66	0.27	1.74	3.30
P_2O_5	0.09	0.03	0.13	0.05	0.06	0.06
LOI	0.58	1.54	0.71	0.14	1.33	0.25
Total	99.81	98.91	99.15	99.45	99.95	99.45
Cr	123	66	103	265	156	158
Mn	467	420	737	1518	989	728
Ni	55	25	15	61	76	18
Cu	24	11	12	21	30	36
Zn	142	66	74	146	118	125
Ga	33	14	23	37	36	36
Rb	174	40	22	6	48	111
Sr	97	29	82	360	143	130
Y	30	25	37	90	53	45
Zr	156	242	78	583	279	265
Nb	19	10	9	85	29	24
Ba	618	373	150	113	1172	887
Pb	25	4	5	4	13	18
Th	13.5	12.1	0.4	7.4	20.9	19.2
Co	26	14	13	45	32	22
V	169	78	109	353	220	211

[a] WR data used for the calculations presented in Section 5.2 and Fig. 16.

investigated rutile-bearing mineral assemblages, but resetting is significant, temperatures have to be treated as minimum values. Sixteen rutile grains with Zr>3800 ppm (apparently representing >900 °C) have been found in 6 different localities (IVZ-R5, R6, R19, R20, R36 and R37). All analyses give low Si signals, excluding contamination from minute zircon inclusions.

While temperature estimates from the IVZ granulite facies rocks based on Fe–Mg exchange are ca. 100 °C lower than results based on rutile thermometry, mineral phase assemblage considerations are broadly consistent with our results. As summarized above, minimum temperatures can be given as 800 °C based on the coexistence of Opx+Kfs as well as the absence of biotite in Grt+Kfs+Sil mineral assemblages with Fe/(Fe+Mg) ratios of 0.6 (see Fig. 2). An independent maximum temperature estimate is difficult to make due to the absence of Mg-Al-rich rocks in the IVZ, where the presence or absence of coexisting Sil+Opx points to temperatures above or below 900 °C, respectively. However, as a final note, we would like to point out that several Kfs-Sil-bearing gneisses are very restitic (sillimanite and garnet-rich), indicating significant melt loss. Schnetger (1994) modeled melt extraction rates of up to 40% based on trace element abundances. Such high melt losses are only achieved in typical metapelites at temperatures above 870 °C at 1.0 GPa (see Fig. 6 in Spear et al., 1999).

5.2. Rutile formation from biotite and expected Nb behavior

As previously presented, textures observed in the studied rocks are evidence for prograde rutile growth associated with the breakdown of high-Ti biotite. With the marked contrast in Nb partitioning between biotite and rutile, we explore in this section how the observed Nb systematics in rutile can be linked to biotite breakdown. The simplified conceptual model (Fig. 15) basically includes four main steps: (1) An initial step where only biotite is present and all Ti and Nb in the system (whole rock) is incorporated in this mineral. (2) An early stage where a few rutile grains exist. Biotite is still the main Ti-carrier (high Bt/Rt ratio). Nb is distributed between both phases. (3) As the reaction continues, the Bt/Rt ratio decreases and rutile becomes the main Ti- and Nb-carrier. (4) The final stage is reached when all biotite is consumed and only rutile is present, incorporating all Ti and Nb of the whole rock.

Combining the crystallization model presented above with exchange coefficients, it is possible to quantitatively model the behavior of Nb through these stages. Klemme et al. (2005) presented experimentally derived rutile/melt partition coefficients for a range of trace elements, including Nb. Combined with Ti partitioning between rutile and melt, an exchange coefficient of the Nb/Ti ratio between rutile and melt can be calculated as 2.47 $K_{D\ Nb/Ti}^{Rt/melt}$; following the terminology of Beattie et al., 1993). The compatible behavior of Nb in rutile compared to melt contrasts strongly with the partitioning behavior of biotite. LaTourrette et al. (1995) found Nb to be incompatible in phlogopite compared to melt, with a $K_{D\ Nb/Ti}^{Bt/melt}$ of 0.050. Neglecting minor differences of melt composition in both studies, we can calculate an exchange coefficient for Nb/Ti between rutile and biotite $K_{D\ Nb/Ti}^{Rt/Bt}$ of 48.7. This compares well with results from sample IVZ-R19e, where a $K_{D\ Nb/Ti}^{Rt/Bt}$ of ca. 60 has been measured (see Fig. 13).

As an example, calculations were carried out for an amphibolite facies garnet–sillimanite–biotite schist from Val Strona (sample IVZ-R17b). Ti concentrations in biotite do not show any systematic variation throughout the upper-amphibolite to granulite facies transition (unpublished EDS and WDS analyses). Therefore, the Ti concentration of biotite was kept constant throughout the calculation steps. Results are graphically depicted in Fig. 16.

As Nb is more compatible in rutile than in biotite, the first rutiles to form have high Nb concentrations. As the reaction continues, and the rutile crystallizes, the remaining biotite has lower Nb contents. It can be seen that during the initial stages of the reaction the decrease of only 3% in the modal proportion of biotite leads to a reduction of one order of magnitude in the Nb concentration of both rutile and biotite. Rutiles formed during later stages of this reaction have low Nb contents and eventually the Nb/Ti ratios in rutile is lower than in the whole rock sample.

These simple calculations imply that rutile grains formed by biotite breakdown are expected to record large variations in Nb concentrations (both inter- and intra-grain). Indeed, the Nb concentration data obtained for the studied rutiles (Fig. 11) show that a large spread in Nb concentrations is displayed by rutiles from the lower grade localities. The Nb behavior in these samples is in agreement with the crystallization model proposed and supports the theory that during continuous formation of rutile from biotite, a high spread in Nb concentration is created. Here, we interpret rutiles with the highest Nb concentrations (up to a factor of 5.5 higher than WR Nb/Ti ratios;

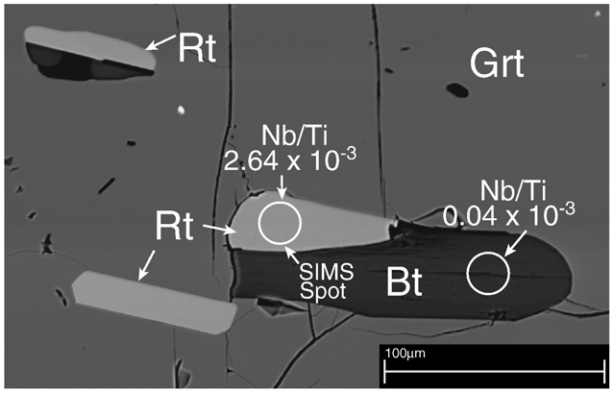

Fig. 13. Nb/Ti ratios (SIMS analyses) of coexisting rutile and biotite occurring in granulite facies metapelitic rocks from the IVZ.

Please cite this article as: Luvizotto, G.L., Zack, T., Nb and Zr behavior in rutile during high-grade metamorphism and retrogression: An example from the Ivrea–Verbano Zone, Chemical Geology (2008), doi:10.1016/j.chemgeo.2008.07.023

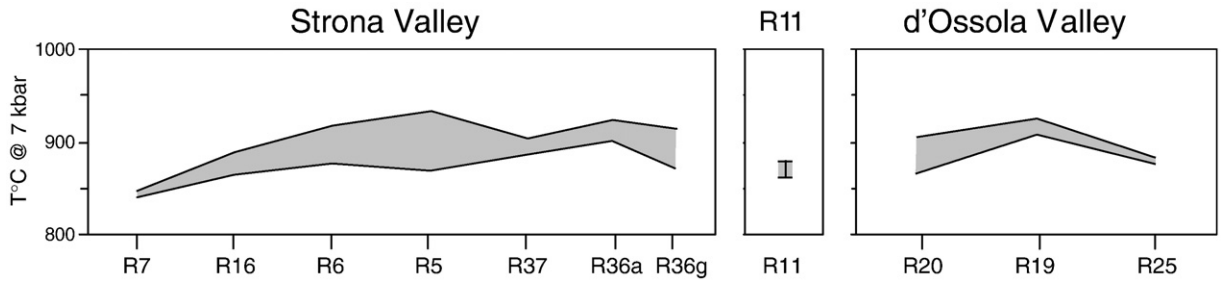

Fig. 14. Temperatures obtained for the studied localities. Shaded area represents the interval delimited by values above the ninetieth percentile. Calculations were based on the Zr content in rutile for a pressure of 7 kbar (calibration of Tomkins et al., 2007).

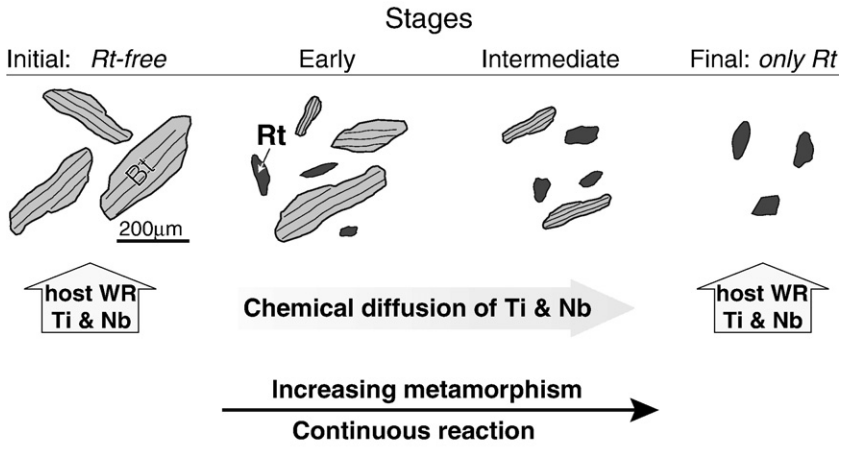

Fig. 15. Illustration showing the four main stages during prograde rutile crystallization from biotite. WR = whole rock chemistry.

see Fig. 12) to be formed first from a biotite-rich mineral assemblage and rutiles with lower Nb concentrations lower than WR Nb/Ti ratios forming last. However, we notice that no pronounced intra-grain variability has been observed in any sample, an observation we cannot satisfactorily explain (see Fig. 9).

In contrast, samples further away from the lowest-grade samples show decreasing variability of Nb in rutile. It can be seen that variability steadily decreases and the average values (diamonds in Fig. 12) approach the WR ratios in the highest grade samples. This observation can be best explained by a homogenization of formerly heterogeneous rutiles during increasing temperature, facilitating dynamic recrystallization, intergrain diffusion and/or communication between rutile grains by a melt phase.

5.3. Post-peak metamorphic processes and their effects on trace element concentrations in rutile

Textures showing rutiles strongly altered by post-peak processes are frequently observed and are characterized not only by corrosion of the rutile grains but also by crystallization of rutile veinlets along K-rich veins (Figs. 7 and 10). In addition, Zr concentrations in rutiles are distinguished by an anomalously large spread and bimodal distribution (Fig. 8).

A dominance of rutiles with Zr concentrations of ca. 1000 ppm is observed for all localities. These rutiles preferentially occur close to or in contact with zircons (Fig. 10). We interpret this as evidence for diffusional resetting related to the slow cooling postulated for the IVZ (see above). We noticed that an apparent temperature of 700 °C (for Zr concentrations of 1000 ppm in rutile) is in surprising agreement to a closure temperature of Zr-in-rutile determined by diffusion experiments (Cherniak et al., 2007). The reequilibration of the Zr content in rutile is favored since zircons are abundant in the rocks, which facilitates ion exchange. We would like to add that with respect to Zr,

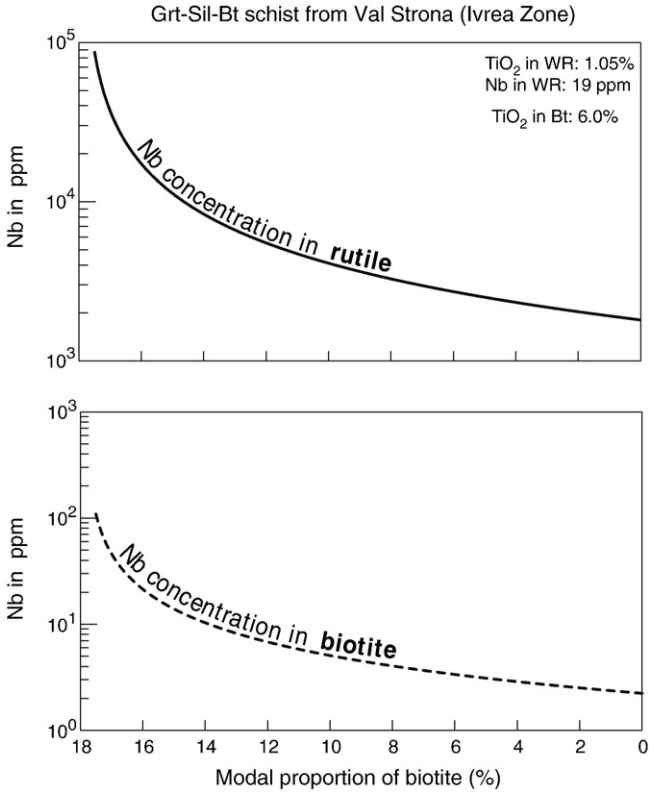

Fig. 16. Quantitative simulation of Nb concentration in rutile and biotite with decreasing modal proportion of biotite. The model reproduces rutile growth in equilibrium with biotite. The calculations were run for an amphibolite facies garnet–sillimanite–biotite schist from Val Strona, (sample IVZ-R17b). The parameters used for the calculations are presented in the diagrams (a complete WR data set is presented in Table 2). Note that Nb concentration is expressed in log scale.

Please cite this article as: Luvizotto, G.L., Zack, T., Nb and Zr behavior in rutile during high-grade metamorphism and retrogression: An example from the Ivrea–Verbano Zone, Chemical Geology (2008), doi:10.1016/j.chemgeo.2008.07.023

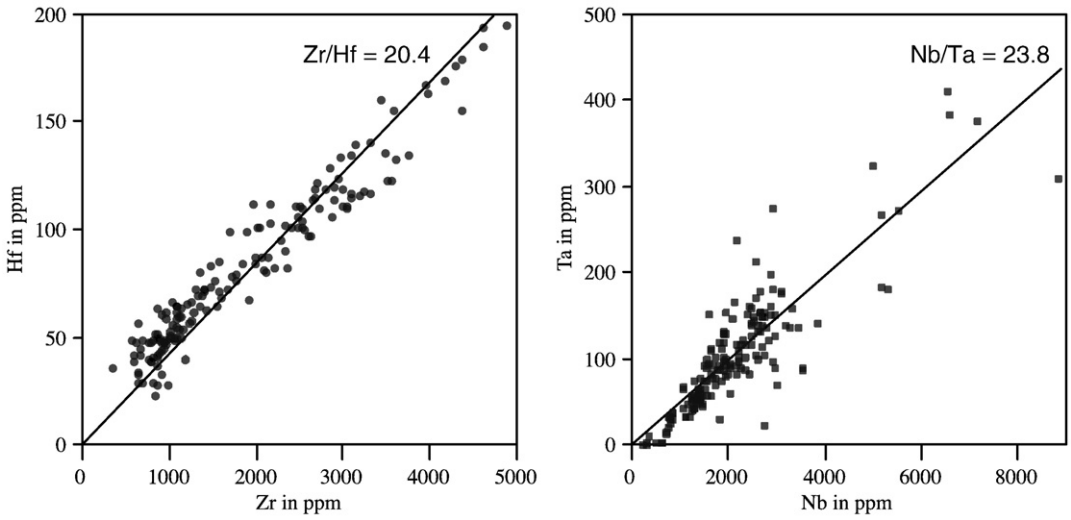

Fig. 17. Diagram showing a strong correlation between Zr and Hf and Nb and Ta in rutiles from IVZ. All data obtained is presented here.

the small variations in zoning and large inter-grain variation (Fig. 9A) are in good agreement with the fluid diffusion controlled regime of Dohmen and Chakraborty (2003, their Fig. 3B). In this regime, transport of an element (in this case Zr) in a fluid is much less efficient than transport within a given mineral (in this case rutile). In contrast, Nb in rutile will not be reset, because no other significant Nb-carrier is available for ion exchange in the investigated samples. This process is also favored by Harley (2008) for ultra-high-temperature rocks from the Napier Complex. The author shows that rutiles occurring adjacent to zircons are zoned with Zr concentrations decreasing from 1100 ppm in the core to 500 ppm in the rim close to adjacent zircon. In addition, Ti concentrations in recrystallized zircon rims are also lower than expected (19–33 ppm Ti). For these data, temperatures obtained by the Zr-in-rutile and the Ti-in-zircon thermometers (Watson et al., 2006) are about 200 °C lower than the peak temperature, overlapping at 775–800 °C. Preliminary results obtained by SIMS in Heidelberg show that, although several zircon grains from our samples seem to record high temperatures (i.e., >900 °C), some grains have rather low Ti concentrations giving apparent temperatures as low as 700 °C (calibration of Watson et al., 2006).

The complex network of veins that cut through the granulite facies mineral assemblage is evidence for post-peak fluid influx. The presence of a fluid phase would only enhance the ion exchange between rutile and zircon. Franz and Harlov (1998) described the presence of extensive networks of K-feldspar micro-veins in the IVZ rocks and suggested a model with intrusion and partial crystallization of the Mafic Complex, with a high-temperature, probably alkali-rich fluid (most likely a concentrated brine) accumulating at the top of the Mafic Complex, and percolating through the overlaying rocks at late stages of emplacement. Although the nature and the exact composition of the fluid are not completely understood, textures and chemical data show that Ti and Zr were mobilized, at least on the thin section scale. This leads to the conclusion that fluids, depending on their composition, can indeed mobilize elements, which are usually assumed to be immobile (e.g., HFSE).

Considering the evidence for both slow cooling and strong fluid ingress, we are left to conclude that both processes could be responsible for the significant resetting of Zr concentrations in the investigated rutiles from the IVZ. Since this is the first study of rutile behavior in slowly cooled granulite facies rocks, it will be insightful to investigate whether or not rutiles in other slowly cooled granulite facies rocks that lack evidence for strong fluid ingress show the same resetting in Zr concentration.

5.4. Behavior of other trace elements

In principle, the same crystallization model proposed for Nb and Ti can also be extended to other trace elements. However, it is important to keep in mind that the modeling will only be valid for elements that are only incorporated in phases involved in the reaction. The same effect observed for Nb is expected to occur for elements with partition coefficients ($D^{\text{Ti-phase/melt}}_{\text{Elem.}}$) significantly different (higher or lower) from those obtained for rutile ($D^{\text{Rt/melt}}_{\text{Elem.}}$). Furthermore, the modeling

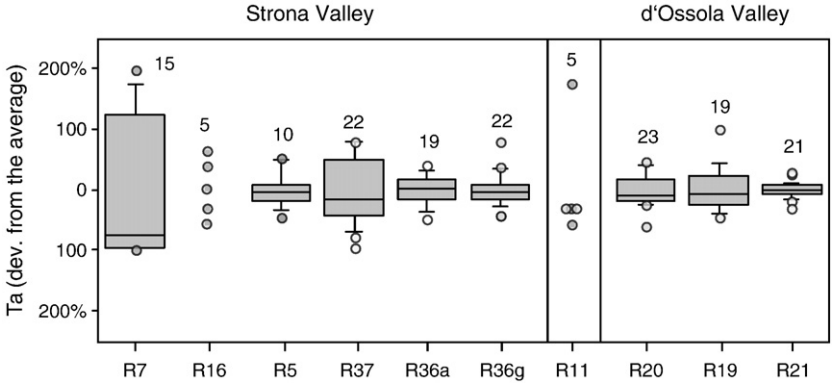

Fig. 18. Variations of Ta content in rutile (SIMS and LA-ICP-MS) through the studied localities. Samples are only plotted for localities with more than 5 analyses.

Please cite this article as: Luvizotto, G.L., Zack, T., Nb and Zr behavior in rutile during high-grade metamorphism and retrogression: An example from the Ivrea–Verbano Zone, Chemical Geology (2008), doi:10.1016/j.chemgeo.2008.07.023

will not be suitable for any trace element that is temperature or pressure dependent (e.g., Zr).

According to our data, no systematic variation is observed for the elements V, Cr, Fe, Sn, Sb and W. However, the same behavior described for Zr and Nb is observed for Hf and Ta, respectively. Hf data show a relatively large spread and a bimodal distribution. Furthermore, a strong correlation between Zr and Hf is observed (Fig. 17), implying that the Hf incorporation in rutiles, at least in our samples, is temperature dependent. This observation may help to target high-Hf rutiles for Hf isotope studies. As for Nb, the spread in Ta concentration is higher in samples from the lower metamorphic grade, and decreases with increasing metamorphism (Fig. 18). This observation is corroborated by the strong correlation between Nb and Ta concentrations in rutile (Fig. 17) and suggests that the crystallization model proposed for Nb can be extended to Ta. Another important conclusion is that the processes that affected the rutiles in the Ivrea Zone rocks were not able to fractionate Zr from Hf and Nb from Ta, at least with respect to rutile. The average Nb/Ta ratio obtained for the studied rutiles (23.8) is slightly higher than the chondritic value (19.9; Münker et al., 2003) but still completely within the scatter of a highly heterogeneous continental crust (at least from 8 to 123; see analyses of crustal rutiles in Supplemental Table of Rudnick et al., 2000).

6. Conclusions

One of the major findings of the present work is that it is possible to couple textures with trace element concentration in accessory phases involved in both prograde and retrograde metamorphic reactions.

The granulite facies metapelitic rocks from the IVZ show a rich inventory of textures and trace element distribution in rutile, making it possible to investigate comprehensively the behavior of important elements (i.e., Ti, Nb, Zr) during metamorphic processes.

Our results show that prograde rutile growth associated with biotite breakdown generates a large spread in Nb concentrations in rutile. After the final stages of the reaction, rutile is the main Ti- and Nb-carrier, and through continuous dynamic recrystallization the Nb concentrations in rutile evolve towards equilibrium reducing the spread in Nb.

Typical textural controls on the Zr concentration in rutile (e.g., inclusion vs. matrix) described in the literature are not observed in our rocks. Additionally, the Zr concentrations are often characterized by a bimodal distribution. Therefore, a new approach where the highest concentration values were statistically selected was applied for the calculation of peak temperatures. For granulites, this method should be preferred against, e.g., calculating temperature from mean Zr concentrations.

Temperatures obtained by the Zr-in-rutile thermometer for the granulite facies rocks are in the range of 850 to 930 °C and are significantly higher than those previously reported in the literature. However, considering that previous calculations were mostly based on Fe–Mg exchange geothermometers and the fact that the late processes that affected the rutiles may also have changed the chemical composition of other primary phases, the high temperatures obtained are not unrealistic. The anomalously large spread in Zr concentrations obtained for the rutiles is interpreted to be related to post-peak diffusional resetting associated with slow cooling rates and/or the presence of fluid.

Another finding of the present work is that fluids can, depending on their compositions, mobilize elements frequently interpreted to be immobile, such as Ti and Zr. This is evidenced by the corrosion of the granulite facies rutile and the crystallization of rutile veinlets associated with textures that suggest late influx of a K-rich fluid. Here we would like to note that HFSE mobility in fluids may be significantly enhanced by the addition of complexing chemical compounds (e.g., Rapp et al., 2008).

Our results encourage further studies in the field of trace element partitioning associated with metamorphic reactions using accessory phases as tools. It also demonstrates the importance of detailed petrographic and textural investigations. Furthermore, our findings spur on the search for other terrains characterized by slow cooling rates in order to evaluate whether the textures and chemical characteristics observed in the IVZ rocks are also present in other localities. This can lead to, e.g., reinterpretations about peak granulite facies temperatures, and element mobility during geological processes.

Acknowledgments

We thank Simon Harley, Yilin Xiao and an anonymous reviewer for their constructive comments that helped to improve the manuscript. Axel Gerdes and Tony Kemp are thanked for inviting us to contribute to this special issue. Hans-Peter Meyer and Thomas Ludwig are thanked for the maintenance of the EMP and SIMS (respectively) at the Mineralogisches Institut, Universität Heidelberg and for their assistance during analyses. Matthias Barth is thanked for his support during LA-ICP-MS analyses in Mainz. Hilmar von Eynatten and Silke Triebold are thanked for fruitful discussions. Renato de Moraes is thanked for his comments and informal review of the manuscript. Emily Whitehurst Zack is thanked for improving the English style and grammar of the manuscript. G. L. Luvizotto would like to thank Andre L. Luvizotto for his help with the MATLAB software and Paula S. Rocha for her support and motivation. This project was financially supported by the Deutsche Forschungsgemeinschaft (projects ZA 285/2 and EY 23/3).

Appendix A. Supplementary data

Supplementary data associated with this article can be found, in the online version, at doi:10.1016/j.chemgeo.2008.07.023.

References

Baldwin, J., Brown, M., Schmitz, M., 2007. First application of titanium-in-zircon thermometry to ultrahigh-temperature metamorphism. Geology 35 (4), 295–298.
Barboza, S.A., Bergantz, G.W., 2000. Metamorphism and anatexis in the mafic complex contact aureole, Ivrea Zone, Northern Italy. Journal of Geology 41 (8), 1307–1327.
Barboza, S.A., Bergantz, G.W., Brown, M., 1999. Regional granulite facies metamorphism in the Ivrea Zone: Is the mafic complex the smoking gun or a red herring? Geology 27 (5), 447–450.
Beattie, P., Drake, M., Jones, J., Leeman, W., Longhi, J., McKay, G., Nielsen, R., Palme, H., Shaw, D., Takahashi, E., Watson, B., 1993. Terminology for trace-element partitioning. Geochimica et Cosmochimica Acta 57, 1605–1606.
Berckhemer, H., 1969. Direct evidence for the composition of the lower crust and moho. Tectonophysics 8, 97–105.
Boriani, A., Origoni, E.G., Borghi, A., Caironi, V., 1990. The evolution of the Serie-dei-Laghi (Strona-Ceneri and Scisti-Deilaghi) — the upper component of the Ivrea–Verbano crustal section — Southern Alps, North Italy and Ticino, Switzerland. Tectonophysics 182 (1–2), 103–118.
Cherniak, D.J., Manchester, J., Watson, E.B., 2007. Zr and Hf diffusion in rutile. Earth and Planetary Science Letters 261, 267–279.
Davis, W.J., 1997. U–Pb zircon and rutile ages from granulite xenoliths in the Slave Province; evidence for mafic magmatism in the lower crust coincident with Proterozoic dike swarms. Geology 25 (4), 343–346.
Deer, W.A., Howie, R., Zussman, J., 1992. An introduction to the rock-forming minerals. Harlow, Essex, England. 696pp.
Demarchi, G., Quick, J.E., Sinigoi, S., Mayer, A., 1998. Pressure gradient and original orientation of a lower-crustal intrusion in the Ivrea–Verbano Zone, Northern Italy. Journal of Geology 106 (5), 609–621.
Dohmen, R., Chakraborty, S., 2003. Mechanism and kinetics of element and isotopic exchange mediated by a fluid phase. American Mineralogist 88, 1251–1270.
Dooley, D.F., Patiño-Douce, A.E., 1996. Fluid-absent melting of F-rich phlogopite plus rutile plus quartz. American Mineralogist 81 (1–2), 202–212.
Fitzsimons, I., Harley, S., 1994. The influence of retrograde cation exchange on granulite *P–T* estimates and a convergence technique for the recovery of peak metamorphic conditions. Journal of Petrology 35 (2), 543–576.
Franz, L., Harlov, D.E., 1998. High-grade K-feldspar veining in granulites from the Ivrea–Verbano Zone, Northern Italy: fluid flow in the lower crust and implications for granulite facies genesis. Journal of Geology 106 (4), 455–472.
Gao, J., John, T., Klemd, R., Xiong, X., 2007. Mobilization of Ti–Nb–Ta during subduction: evidence from rutile-bearing dehydration segregations and veins hosted in eclogite, Tianshan, NW China. Geochimica et Cosmochimica Acta 71 (20), 4974–4996.

Graham, J., Morris, R., 1973. Tungsten- and antimony-substituted rutile. Mineralogical Magazine 39, 470–473.

Haggerty, S.E., 1991. Oxide mineralogy of the upper mantle. In: Lindsley, D.H. (Ed.), Oxide mineralogy minerals: Petrological and magnetic significance.

Handy, M.R., Franz, L., Heller, F., Janott, B., Zurbriggen, R., 1999. Multistage accretion and exhumation of the continental crust (Ivrea crustal section, Italy and Switzerland). Tectonics 18 (6), 1154–1177.

Harley, S., 1989. The origins of granulites; a metamorphic perspective. Geological Magazine 126 (3), 215–247.

Harley, S.L., 2008. Refining the *P–T* records of UHT crustal metamorphism. Journal of Metamorphic Geology 26 (2), 125–154.

Hayden, L.A., Watson, E.B., Wark, D.A., 2007. A thermobarometer for sphene (titanite). Contributions to Mineralogy and Petrology 155 (4), 529–540.

Henk, A., Franz, L., Teufel, S., Oncken, O., 1997. Magmatic underplating, extension, and crustal reequilibration: insights from a cross-section through the Ivrea Zone and Strona–Ceneri Zone, northern Italy. Journal of Geology 105 (3), 367–377.

Henry, D.J., Guidott, C.V., 2002. Titanium in biotite from metapelitic rocks: temperature effects, crystal-chemical controls, and petrologic applications. American Mineralogist 87 (4), 375–382.

Henry, D.J., Guidotti, C.V., Thomson, J.A., 2005. The Ti-saturation surface for low-to-medium pressure metapelitic biotites: implications for geothermometry and Ti-substitution mechanisms. American Mineralogist 90 (2–3), 316–328.

Kelsey, D., Clark, C., Hand, M., 2008. Thermobarometric modelling of zircon and monazite growth in melt-bearing systems: examples using model metapelitic and metapsammitic granulites. Journal of Metamorphic Geology 26 (2), 199–212.

Klemme, S., Prowatke, S., Hametner, K., Gunther, D., 2005. Partitioning of trace elements between rutile and silicate melts: implications for subduction zones. Geochimica et Cosmochimica Acta 69 (9), 2361–2371.

Köppel, V., 1974. Isotopic U–Pb ages of monazites and zircons from crust–mantle transition and adjacent units of Ivrea and Ceneri Zones (Southern-Alps, Italy). Contributions to Mineralogy and Petrology 43 (1), 55–70.

Kretz, R., 1983. Symbols for rock forming minerals. American Mineralogist 68 (1–2), 277–279.

LaTourrette, T., Hervig, R.L., Holloway, J.R., 1995. Trace-element partitioning between amphibole, phlogopite, and basanite melt. Earth and Planetary Science Letters 135 (1–4), 13–30.

Li, Q., Li, S., Zheng, Y.F., Li, H., Massonne, H.J., Wang, Q., 2003. A high precision U–Pb age of metamorphic rutile in coesite-bearing eclogite from the Dabie Mountains in central China: a new constraint on the cooling history. Chemical Geology 200 (3–4), 255–265.

Luvizotto, G., Zack, T., Meyer, H., Ludwig, T., Triebold, S., Kronz, A., Münker, C., Stockli, D., Prowatke, S., Klemme, S., Jacob, D.E., von Eynatten, H., , this issue. Rutile crystals as potential secondary standards for microanalysis. Chemical Geology.

Meinhold, G., Anders, B., Kostopoulos, D., Reischmann, T., 2008. Rutile chemistry and thermometry as provenance indicator: an example from Chios Island, Greece. Sedimentary Geology 203, 98–111.

Mezger, K., Hanson, G.N., Bohlen, S.R., 1989. High-precision U–Pb ages of metamorphic rutile: application to the cooling history of high-grade terranes. Earth and Planetary Science Letters 96 (1–2), 106–118.

Mezger, K., Essene, E.J., Vanderpluijm, B.A., Halliday, A.N., 1993. U–Pb geochronology of the grenville orogen of Ontario and New York: constraints on ancient crustal tectonics. Contributions to Mineralogy and Petrology 114 (1), 13–26.

Miller, C., Zanetti, A., Thoni, M., Konzett, J., 2007. Eclogitisation of gabbroic rocks: redistribution of trace elements and Zr in rutile thermometry in an Eo-Alpine subduction zone (Eastern Alps). Chemical Geology 239 (1–2), 96–123.

Münker, C., Pfänder, J., Weyer, S., Buchl, A., Kleine, T., Mezger, K., 2003. Evolution of planetary cores and the earth–moon system from Nb/Ta systematics. Science 301, 84–87.

Patiño-Douce, A.E., 1993. Titanium substitution in biotite an empirical model with applications to thermometry, O_2 and H2O barometries, and consequences for biotite stability. Chemical Geology 108 (1–4), 133–162.

Patiño-Douce, A.E., Beard, J.S., 1995. Dehydration-melting of biotite gneiss and quartz amphibolite from 3 to 15 kbar. Journal of Petrology 36 (3), 707–738.

Pattison, D., Begin, N., 1994. Zoning patterns in orthopyroxene and garnet in granulites: implications for geothermometry. Journal of Metamorphic Geology 12 (4), 387–410.

Pattison, D.R.M., Chacko, T., Farquhar, J., McFarlane, C.R.M., 2003. Temperatures of granulite-facies metamorphism: constraints from experimental phase equilibria and thermobarometry corrected for retrograde exchange. Journal of Petrology 44 (5), 867–900.

Pearce, J.A., Cann, J.R., 1973. Tectonic setting of basic volcanic rocks determined using trace element analysis. Earth and Planetary Science Letters 19, 290–300.

Peressini, G., Poller, U., Todt, W., Quick, J.E., Sinigoi, S., Sbisa, A., 2002. Age of magmatism in the Ivrea Zone, NW Italy: a zircon study to test the emplacement model. Geochimica et Cosmochimica Acta 66 (15A), A590.

Peressini, G., Quick, J.E., Sinigoi, S., Hofmann, A.W., Fanning, M., 2007. Duration of a large mafic intrusion and heat transfer in the lower crust: a shrimp U–Pb zircon study in the Ivrea–Verbano Zone (Western Alps, Italy). Journal of Petrology 48 (6), 1185–1218.

Rapp, J., Klemme, S., Harley, S.L., 2008. Experimental studies on rutile solubility. Geochimica et Cosmochimica Acta 72 (12), A776.

Rasmussen, B., 2005. Zircon growth in very low grade metasedimentary rocks: evidence for Zirconium mobility at similar to 250 °C. Contributions to Mineralogy and Petrology 150 (2), 146–155.

Rice, C., Darke, K., Still, J., 1998. Tungsten-bearing rutile from the Kori Kollo gold mine Bolívia. Mineralogical Magazine 62, 421–429.

Rivalenti, G., Garuti, G., Rossi, A., Siena, F., Sinigoi, S., 1981. Existence of different peridotite types and of a layered igneous complex in the Ivrea Zone of the Western Alps. Journal of Petrology 22 (1), 127–153.

Rivalenti, G., Mazzucchelli, M., Barbieri, M.A., Parenti, M., Schmid, R., Zanetti, A., 1997. Garnetite-forming processes in the deep crust: the Val Fiorina case study (Ivrea–Verbano Zone, NW Alps). European Journal of Mineralogy 9 (5), 1053–1071.

Rudnick, R.L., Barth, M., Horn, I., McDonough, W.F., 2000. Rutile-bearing refractory eclogites: missing link between continents and depleted mantle. Science 287 (5451), 278–281.

Rutter, E., Brodie, K., James, T., Burlini, L., 2007. Large-scale folding in the upper part of the Ivrea–Verbano Zone, NW Italy. Journal of Structural Geology 29 (1), 1–17.

Schmid, S.M., Wood, B.J., 1976. Phase relationships in granulitic metapelites from the Ivrea–Verbano Zone (Northern Italy). Contributions to Mineralogy and Petrology 54, 255–279.

Schmid, S.M., Zingg, A., Handy, M., 1987. The kinematics of movements along the insubric line and the emplacement of the Ivrea Zone. Tectonophysics 135 (1–3), 47–66.

Schnetger, B., 1994. Partial melting during the evolution of the amphibolite-facies to granulite-facies gneisses of the Ivrea Zone, Northern Italy. Chemical Geology 113 (1–2), 71–101.

Sills, J.D., 1984. Granulite facies metamorphism in the Ivrea Zone, NW Italy. Schweizerische Mineralogische und Petrographische Mitteilungen 64, 169–191.

Sills, J.D., Tarney, J., 1984. Petrogenesis and tectonic significance of amphibolites interlayered with meta-sedimentary gneisses in the Ivrea Zone, Southern Alps, Northwest Italy. Tectonophysics 107 (3–4), 187–206.

Smith, D., Persil, E.A., 1997. Sb-rich rutile in the manganese concentrations at St. Marcel-Praborna, Aosta Valley, Italy; petrology and crystal chemistry. Mineralogical Magazine 61 (5), 655–669.

Spear, F.S., 1995. Metamorphic phase equilibria and pressure-temperature-time paths. Mineralogical Society of America Monograph. Mineralogical Society of America Washington, D.C., 799p.

Spear, F.S., Kohn, M.J., Cheney, J.T., 1999. *P–T* paths from anatectic pelites. Contributions to Mineralogy and Petrology 134 (1), 17–32.

Spear, F.S., Wark, D.A., Cheney, J.T., Schumacher, J.C., Watson, E.B., 2006. Zr-in-rutile thermometry in blueschists from Sifnos, Greece. Contributions to Mineralogy and Petrology 152 (3), 375–385.

Stendal, H., Toteu, S.F., Frei, R., Penaye, J., Njel, U.O., Bassahak, J., Nni, J., Kankeu, B., Ngako, V., Hell, J.V., 2006. Derivation of detrital rutile in the Yaounde region from the Neoproterozoic Pan-African belt in southern Cameroon (Central Africa). Journal of African Earth Sciences 44, 443–458.

Tomkins, H.S., Powell, R., Ellis, D.J., 2007. The pressure dependence of the Zirconium-in-rutile thermometer. Journal of Metamorphic Geology 25 (6), 703–713.

Triebold, S., von Eynatten, H., Luvizotto, G.L., Zack, T., 2007. Deducing source rock lithology from detrital rutile geochemistry: an example from the Erzgebirge, Germany. Chemical Geology 244 (3–4), 421–436.

Vavra, G., Schaltegger, U., 1999. Post-granulite facies monazite growth and rejuvenation during Permian to Lower Jurassic thermal and fluid events in the Ivrea Zone (Southern Alps). Contributions to Mineralogy and Petrology 134 (4), 405–414.

Vavra, G., Gebauer, D., Schmid, R., Compston, W., 1996. Multiple zircon growth and recrystallization during polyphase Late Carboniferous to Triassic metamorphism in granulites of the Ivrea Zone (Southern Alps): an ion microprobe (SHRIMP) study. Contributions to Mineralogy and Petrology 122 (4), 337–358.

Vry, J.K., Baker, J.A., 2006. LA-MC-ICPMS Pb–Pb dating of rutile from slowly cooled granulites: confirmation of the high closure temperature for Pb diffusion in rutile. Geochimica et Cosmochimica Acta 70 (7), 1807–1820.

Wark, D.A., Watson, E.B., 2006. TitaniQ: a titanium-in-quartz geothermometer. Contributions to Mineralogy and Petrology 152, 743–754.

Watson, E.B., Wark, D.A., Thomas, J.B., 2006. Crystallization thermometers for zircon and rutile. Contributions to Mineralogy and Petrology 151, 413–433.

White, R.W., Powell, R., Holland, T.J.B., 2007. Progress relating to calculation of partial melting equilibria for metapelites. Journal of Metamorphic Geology 25 (5), 511–527.

Zack, T., Luvizotto, G.L., 2006. Application of rutile thermometry to eclogites. Mineralogy and Petrology 88 (1), 69–85.

Zack, T., Kronz, A., Foley, S.F., Rivers, T., 2002. Trace element abundances in rutiles from eclogites and associated garnet mica schists. Chemical Geology 184 (1–2), 97–122.

Zack, T., Moraes, R., Kronz, A., 2004a. Temperature dependence of Zr in rutile: empirical calibration of a rutile thermometer. Contributions to Mineralogy and Petrology 148, 471–488.

Zack, T., von Eynatten, H., Kronz, A., 2004b. Rutile geochemistry and its potential use in quantitative provenance studies. Sedimentary Geology 171 (1), 37–58.

Zingg, A., 1980. Regional metamorphism in the Ivrea Zone (Southern Alps, N-Italy): field and microscopic investigations. Schweizerische Mineralogische und Petrographische Mitteilungen 60, 153–179.

Zingg, A., 1983. The Ivrea and Strona-Ceneri zones (Southern Alps, Ticino and N, Italy) — a review. Schweizerische Mineralogische und Petrographische Mitteilungen 63, 361–392.

Zingg, A., Handy, M.R., Hunziker, J.C., Schmid, S.M., 1990. Tectonometamorphic history of the Ivrea Zone and its relationship to the crustal evolution of the Southern Alps. Tectonophysics 182 (1–2), 169–192.

Please cite this article as: Luvizotto, G.L., Zack, T., Nb and Zr behavior in rutile during high-grade metamorphism and retrogression: An example from the Ivrea–Verbano Zone, Chemical Geology (2008), doi:10.1016/j.chemgeo.2008.07.023